Solar Energetic Emission and Particles Explorer (SEEPE)

Siming Liu
Purple Mountain Observatory

Paolo Soffitta
IAPS/INAF

Ronaldo Bellazzini, INFN-Pisa
Robert Wimmer-Schweingruber, CAU Kiel
Valentina Zharkova, Northumbria University, UK
Yong Liu, NSSC, China

Scientific Motivation

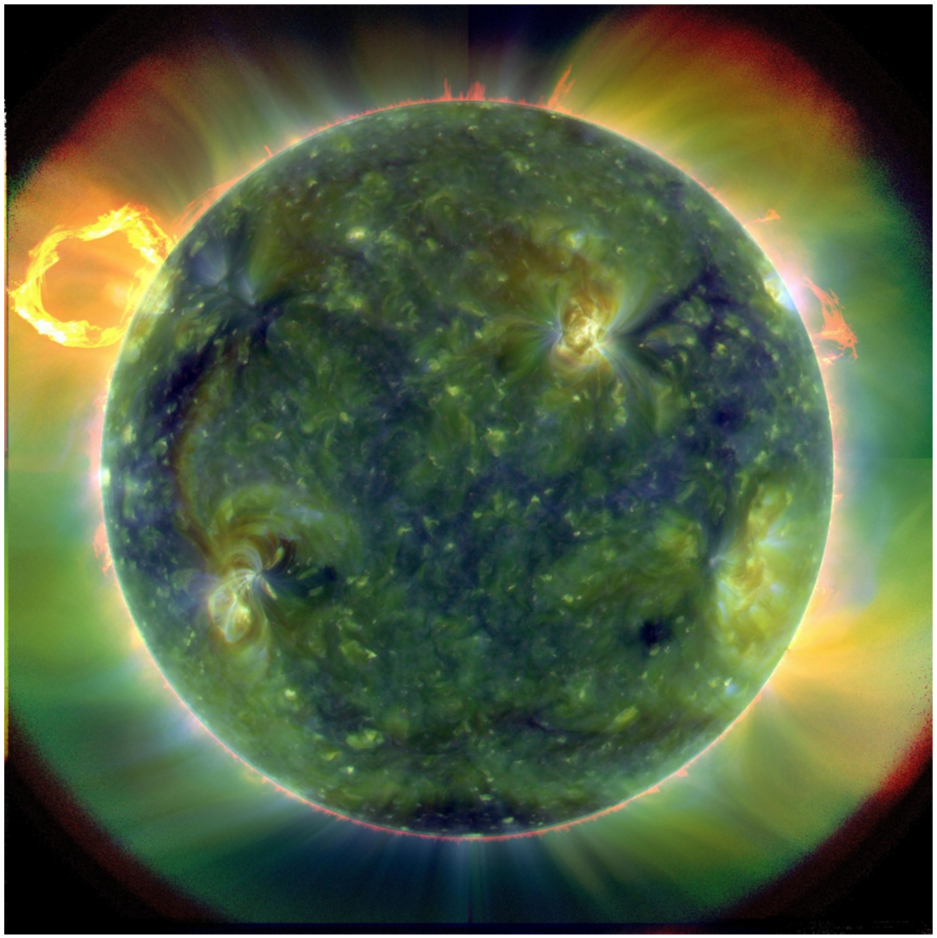

Solar Magnetic Fields

↓

Magnetic Reconnection

↓

Flare, CME, Solar Wind

↓

Space Weather

Observations of energetic emission in solar flares → relativistic particles

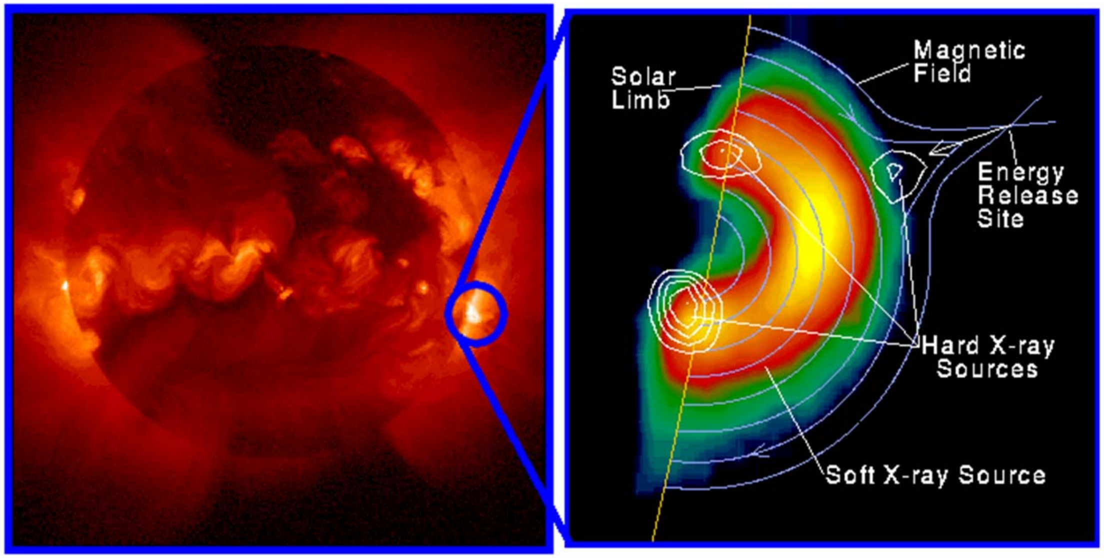

Yohkoh X-ray Image of a Solar Flare, Combined Image in Soft X-rays (left) and Soft X-rays with Hard X-ray Contours (right). Jan 13, 1992.

•Large numbers of non-thermal ions and electrons produced in flares

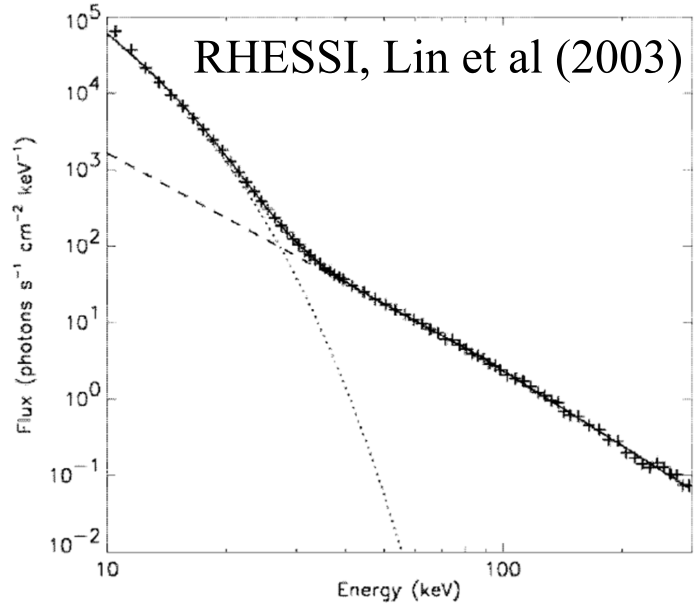

• Magnetic reconnection is a fundamental process of energy release in solar flares

•This process can account for generation of relativistic particles with power law energy distributions

•This process ejects highly directed particles along magnetic field direction

Scientific Motivation

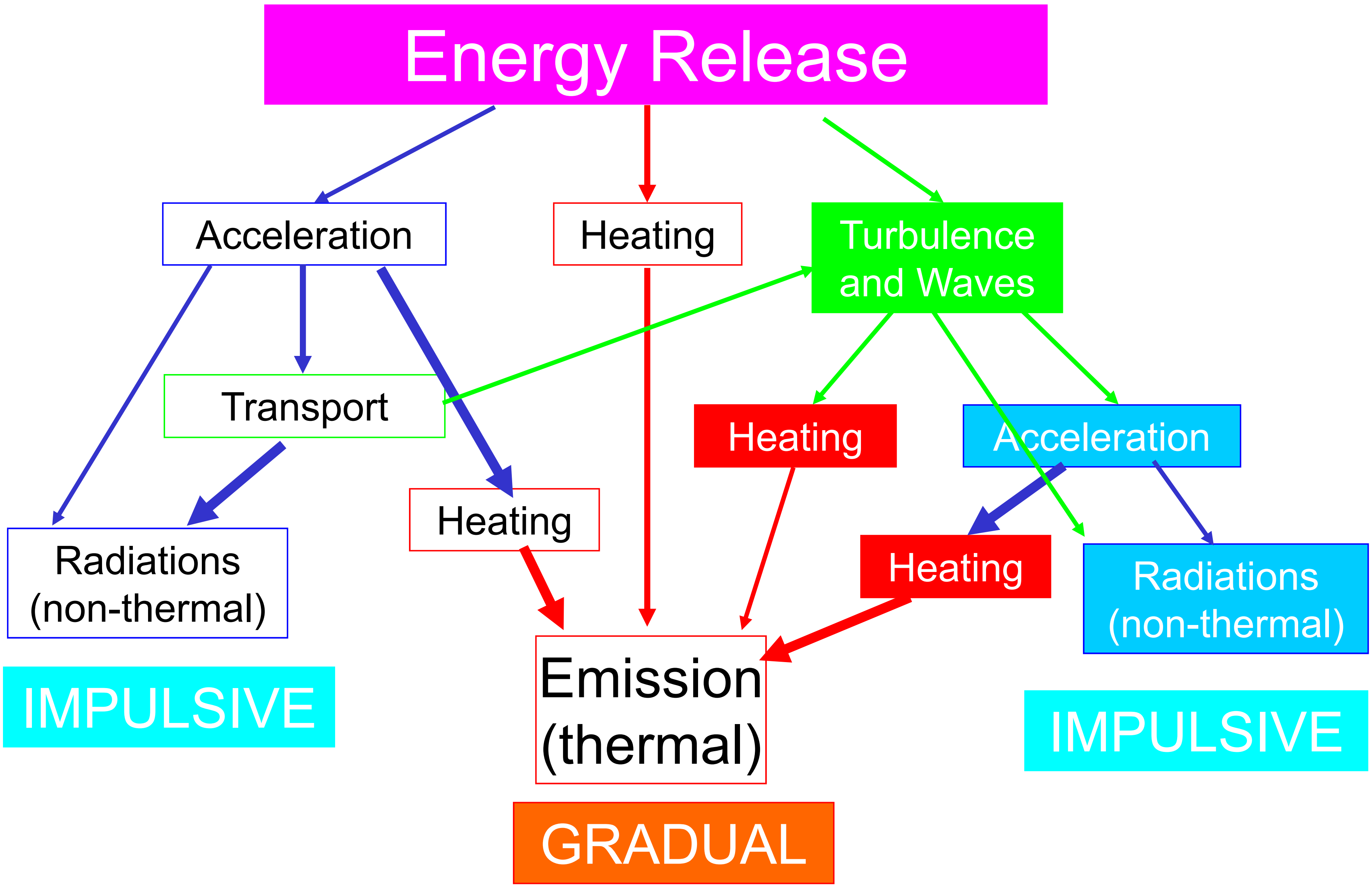

PARTICLE PRECIPITATION

Zharkova et al. (2010) using Fokker-Plank equation for the evolution of electron distribution and using bremsstrahlung cross-section tackled the problem of deriving Hard X-ray spectrum, directivity and polarization of solar flares

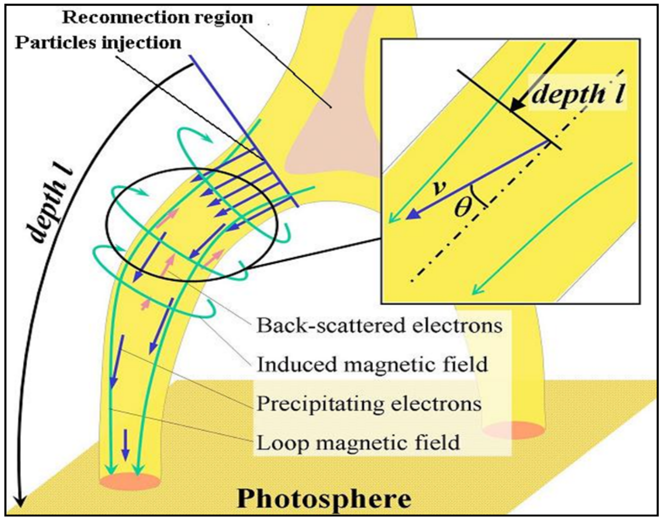

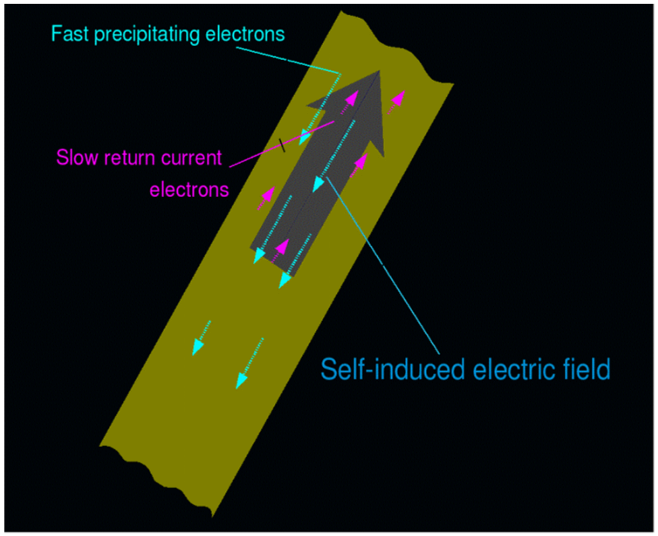

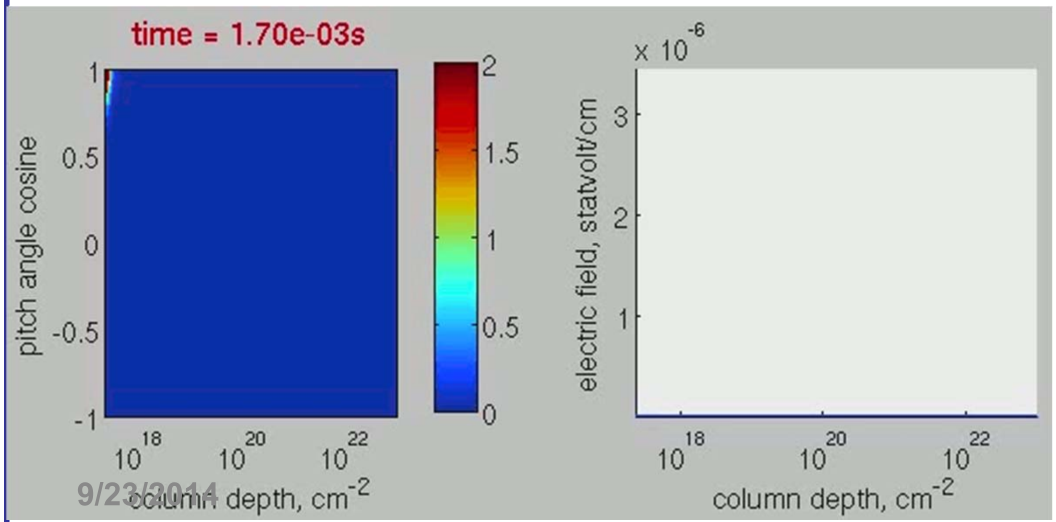

Taking into account :

1. **Collision loss**
2. **Self-induced electric field** (Ohmic losses)
3. **Converging magnetic field** (loss cone)

Returning electrons are present (negative cosine) mostly due to (2) and (3) effects (see cartoon).

Evolution of the directivity and polarization degree at 30 keV and 100 keV for soft ($\gamma = 7$) and hard ($\gamma = 3$) electron beam for different pitch (emission) angle of photons

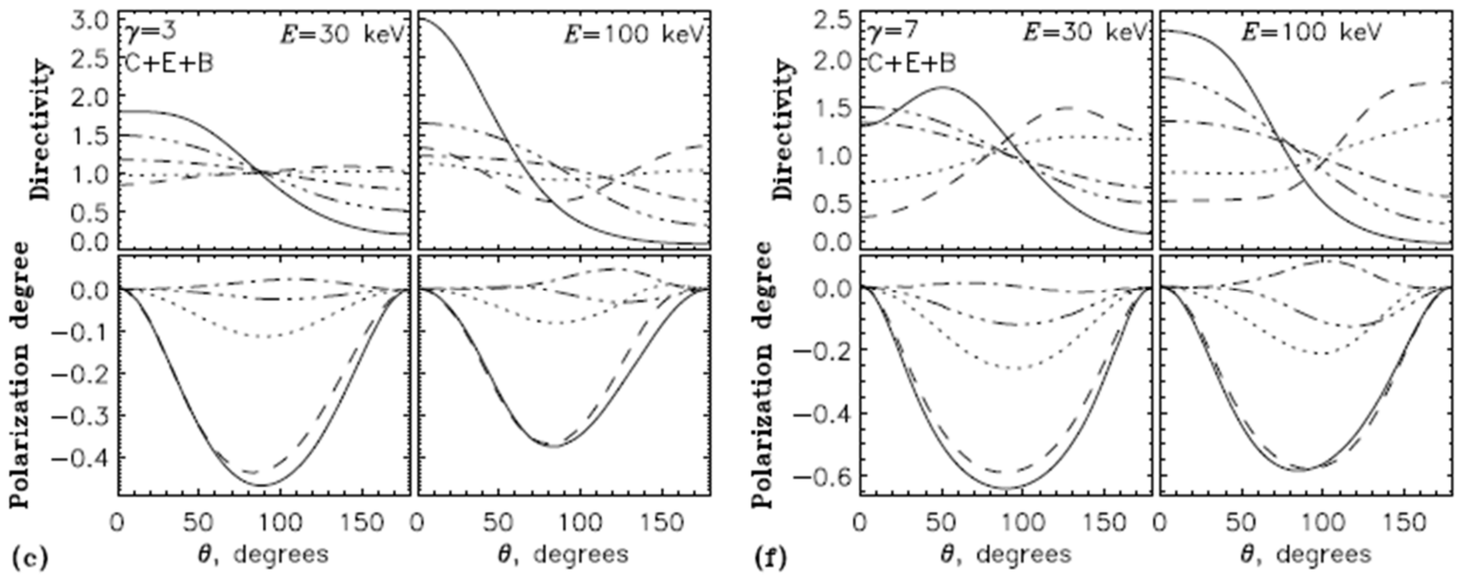

Solid = 0, Dashed = 10^{18} cm^{-2}, Dotted = 10^{19} cm^{-2}, Dash-Dotted = 10^{20} cm^{-2}, Dash-Double Dotted = 10^{21} cm^{-2}

- **Intensity is mostly directed down-ward for hard electron spectrum while it evolves upward for soft electron spectrum due to return current.**
- **Polarization is highest for $\vartheta = 90^o$ it decreases at large depth due to randomization.**
- **Not shown but the evolution with depth of polarization and directivity depends on the model of precipitation assumed.**

Intensity and polarization spectrum of the whole flare for soft and hard electron beam.

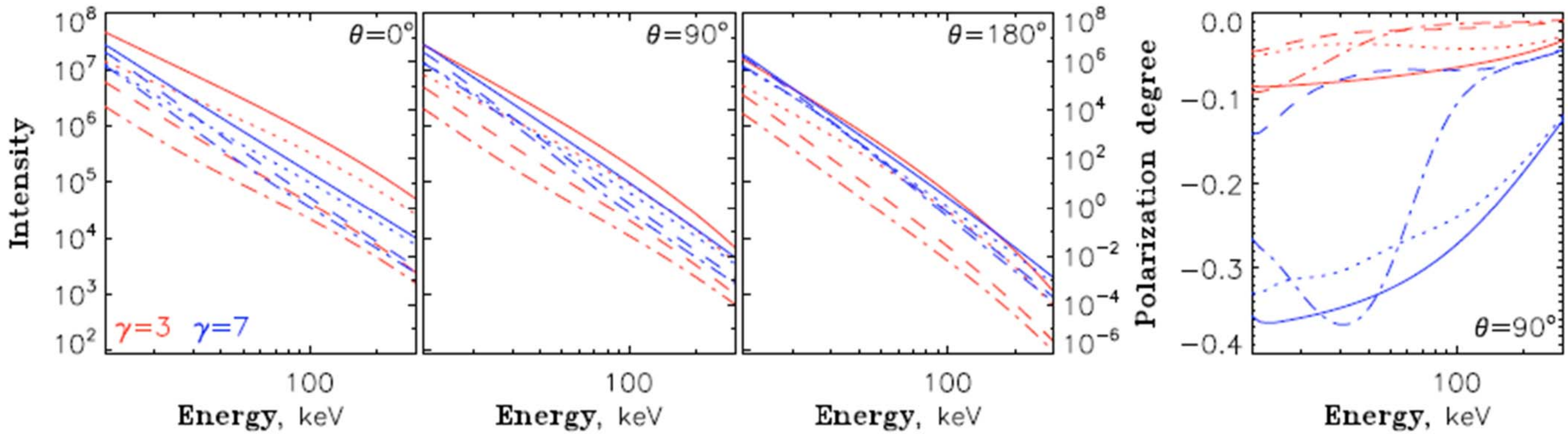

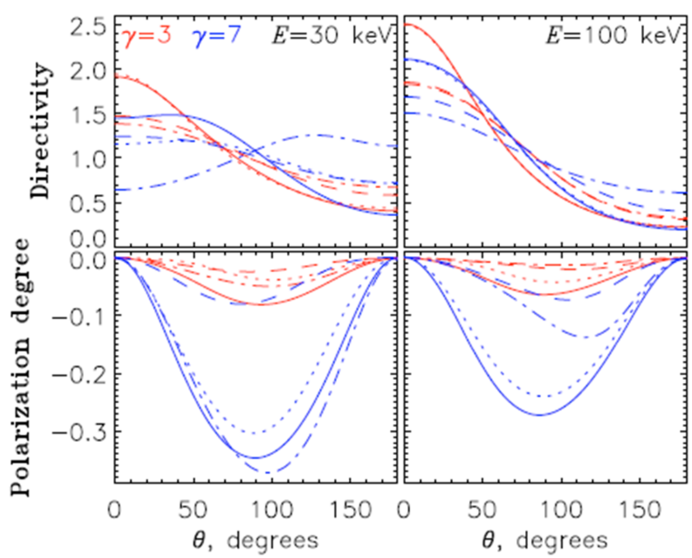

Solid : Collision; **dotted** collision and return current;
Dashed : Collision and converging magnetic beam
Dash-dotted : all

- Energy dependent polarization measurement helps to disentangle between precipitation models and electron beam hardness.
- Energy breaks in the intensity spectrum helps to further constrain beam hardness.
- Maximum of polarization is reached at low energy for soft beam and when the flare is on the limb $\vartheta = 90^o$.

Current observational status and direction for an ESA-CAS small mission.

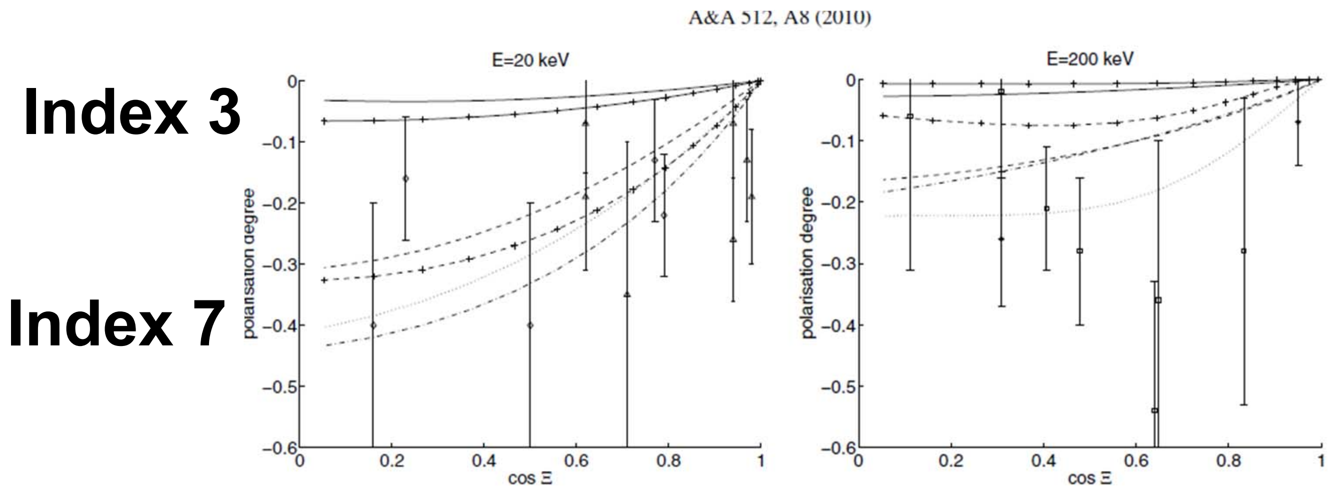

Zharkova et al applied their modeling to measurements of Tindo 1970,1972, Tramiel et al., (1984) , Suarez-Garcia (2006), Boggs(2006) .

However :

- Present measurements have low significance mostly due to the sensitivity and threshold of the instruments flown up-to now. Much more precision for measurements across the whole sun disk are needed to constrain models and to determine the plasma parameters.
- Measurements resolved in energy are very desirable The energy band 15-35 keV looks promising because of the larger polarization and flux expected.
- Time resolved polarimetry finally would allow to study the evolution. However the necessary time resolution may be in contrast with the large number of counts needed for a sensitive measurement placing constraints on the collecting area needed.

Scientific Motivation

Low-energy: Gradual Thermal Coronal Source

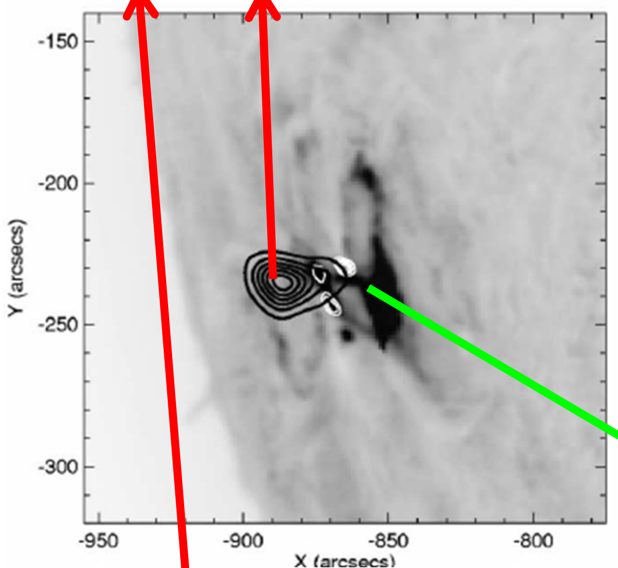

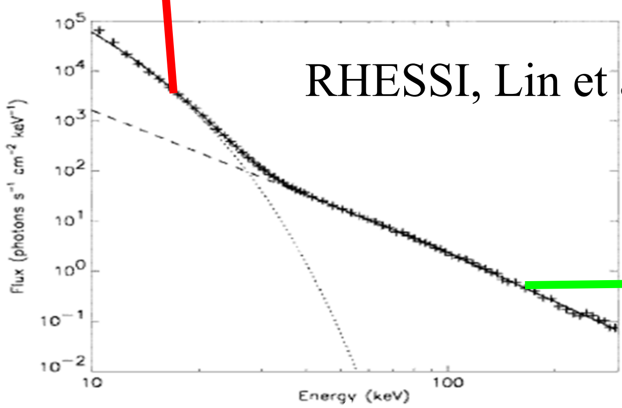

RHESSI, Lin et al (2003)

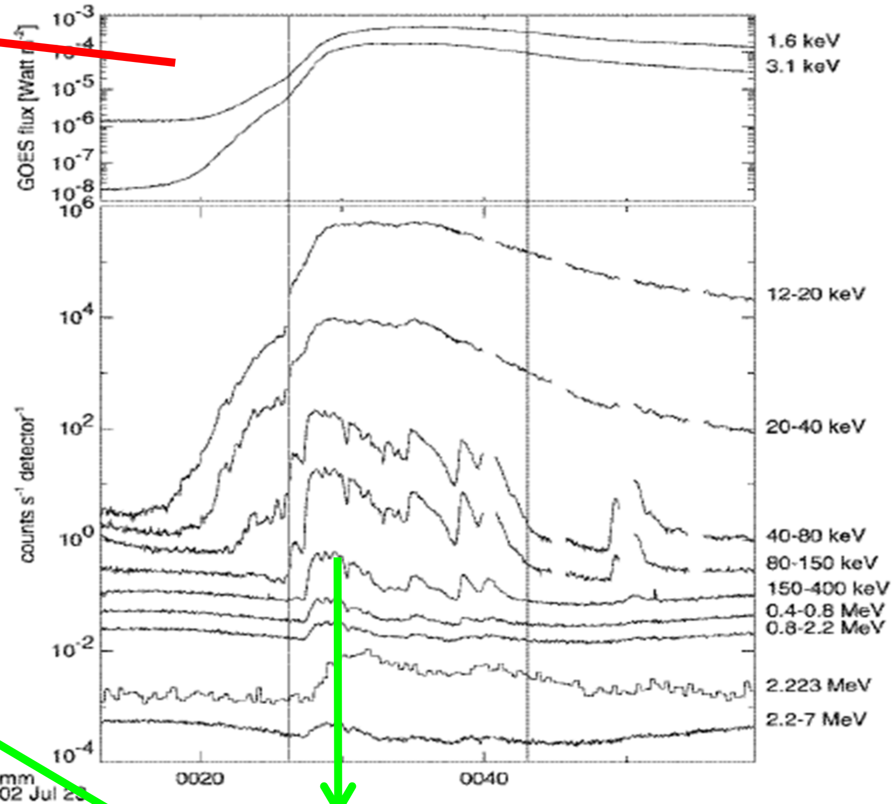

High-Energy: Impulsive Non-thermal Chromospheric Footpoints

Scientific Aim

To explore the magnetic energy release and consequent plasma heating and particle acceleration in the solar atmosphere by distinguishing the thermal and the non-thermal emission component:

	Thermal	Non-thermal
Temporal	**Gradual**	**Impulsive**
Spectral	**Exponential**	**Power-Law**
Polarization	**Isotropic**	**Polarized**
Transport	**Local**	**Global**

Scientific Payload

High Energy Burst Spectrometer (HEBS)

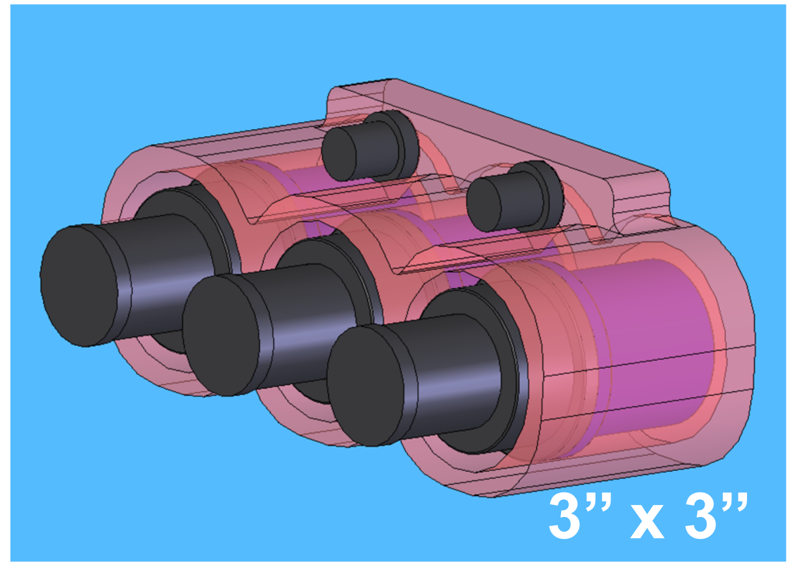

Size	362×349×172.5mm
Weight	20.5 kg
Power	20 W
Energy Range	10keV - 600MeV
Energy Resolution	3%@662keV
Temporal Resolution	1s(quiescent),32ms (flare-mode)

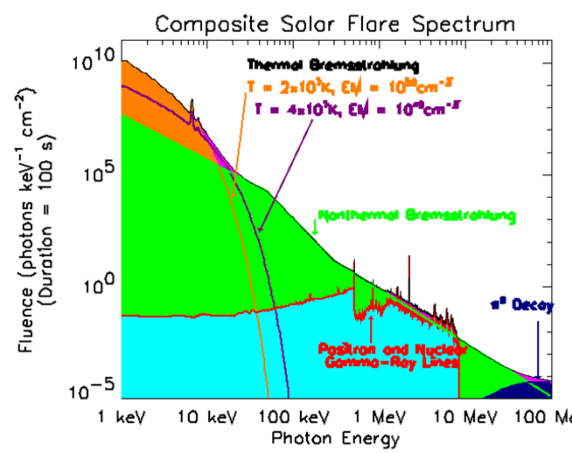

It is a possible GRB detector (area = 0.55 of Fermi GBM/BGO)

Scientific Payload

Institute for Space Astrophysics and Planetology
Istituto di Astrofisica e Planetologia Spaziali

A solar flares X-ray polarimeter

S. Fabiani[1,3], R. Bellazzini[2], F. Berrilli[3], A. Brez[2], E. Costa[1], F. Muleri[1], M. Pinchera[2], A. Rubini[1], P. Soffitta[1], and G. Spandre[2]

$$\mathrm{MDP} = \frac{4.29}{\mu \cdot R} \cdot \sqrt{\frac{R+B}{T}}$$

Flare Class	MDP (%)	Integration Time (s)
X10	0.6	748
X5.1	1.3	989
X1.2	4.8	239
M5.2	6.6	489
M1	46.4	128

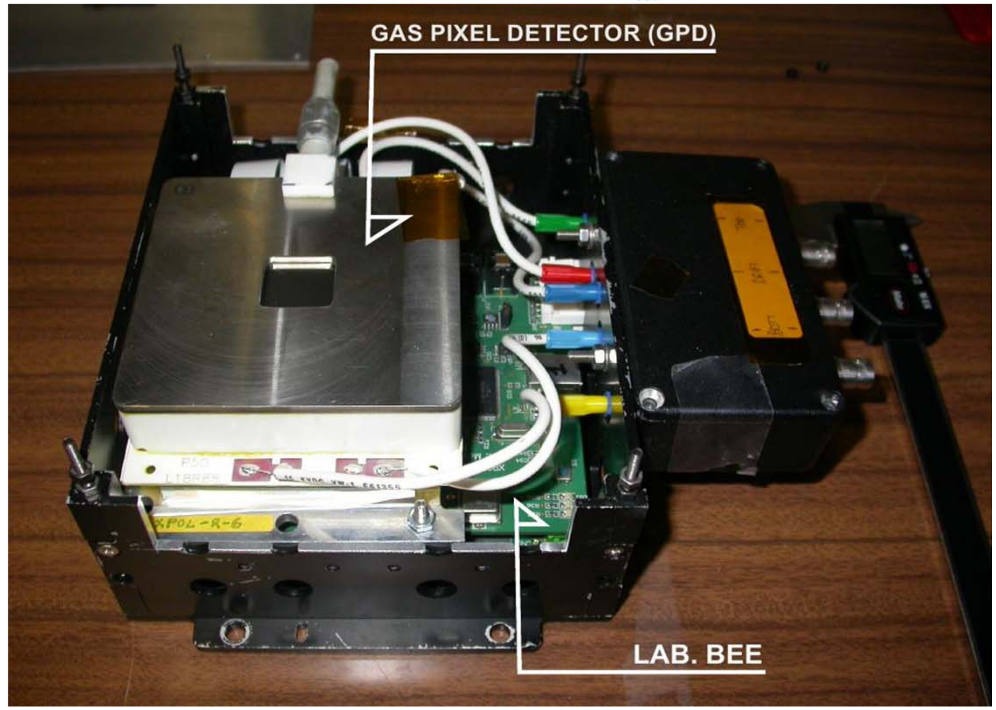

X-ray Polarimeter (Polarization)

Weight	16 kg
Power	25 W
Energy Range	10-35keV(for non-thermal bremsstrahlung)

Fundamental parameters

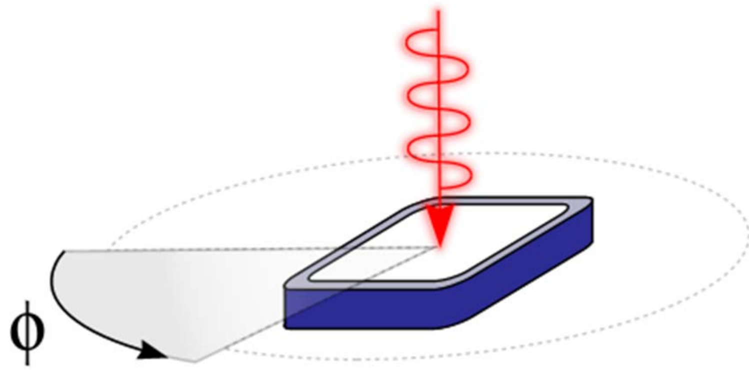

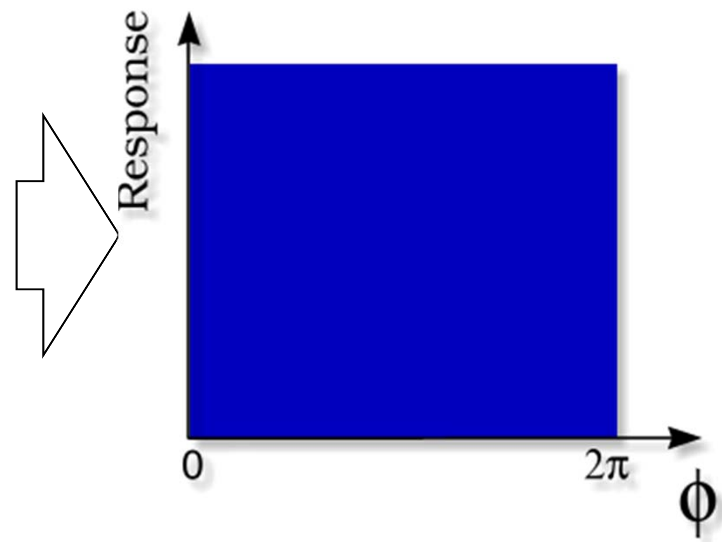

Every polarimeter is composed of
(1) an analyzer, a stage where an interaction occurs, whose outcome angle depends on polarization, and (2) a detector of the products of the interaction, capable to measure their angular distribution.

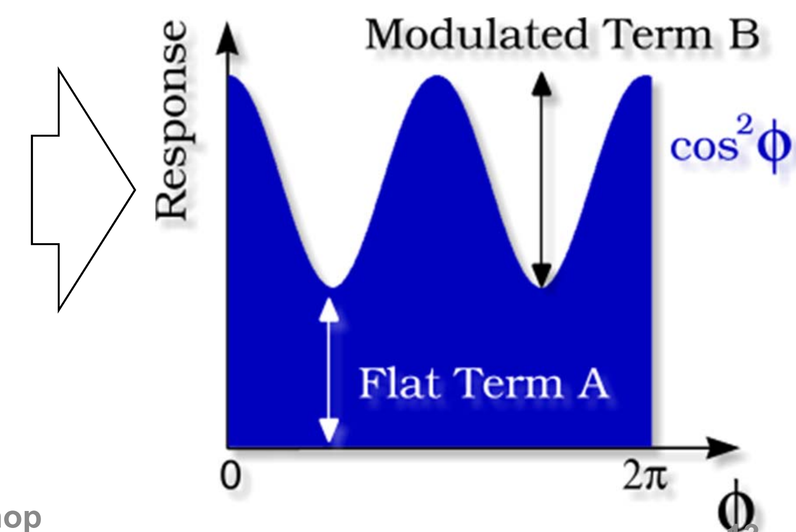

Fundamental parameters

Fit function:

$$\mathcal{M}(\phi) = A + B\cos^2(\phi - \phi_0)$$

$$\frac{\mathcal{M}_{\max} - \mathcal{M}_{\min}}{\mathcal{M}_{\max} + \mathcal{M}_{\min}} = \frac{B}{B + 2A}$$

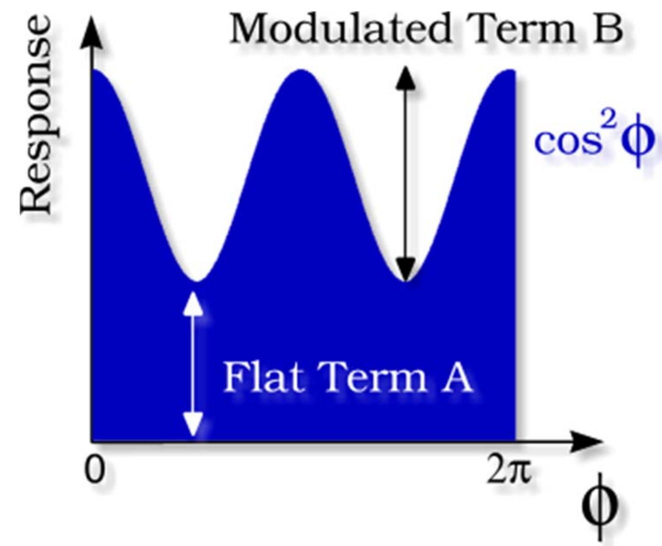

Polarization: $\frac{1}{\mu}\frac{B}{B + 2A}$

μ is the modulation factor, i.e. the modulation for 100% polarized radiation

The level at which it is possible to reject the hypothesis of a non-polarized source at the 99 % confidence level is the Minimum Detectable Polarization (MDP) which measures the sensitivity to a given source in a given observing time T :

$$MDP = \frac{4.29}{\mu S}\sqrt{\frac{(S+B)}{T}}$$

99 % confidence level.

[B] **Background counting rate**
(collimation, good background rejection or small polarimeters in focal plane, high collecting/ active area)

[μ] **Modulation factor**
(max =1, Bragg, Thomson at 90°, Photoelectric effect)

[S] **Source Counting Rate**
(large area or large collector, strong sources)

[T] **Observing Time**
(typical unit is 10^5 s)

X-ray polarimetry with a Gas Pixel Detector

A photon crosses a Beryllium window and it is absorbed in the gas gap, the photoelectron produces a track. The track drifts toward the multiplication stage that is the GEM (Gas Electron Multiplier) which is a insulator foil metallized on both side and perforated by microscopic holes (30 um diameter, 50 um pitch) and it is then collected by the pixellated anode plane that is the upper layer of an ASIC chip.

1-cm drift, 1-bar.
He-DME (20-80) 2-10 keV.

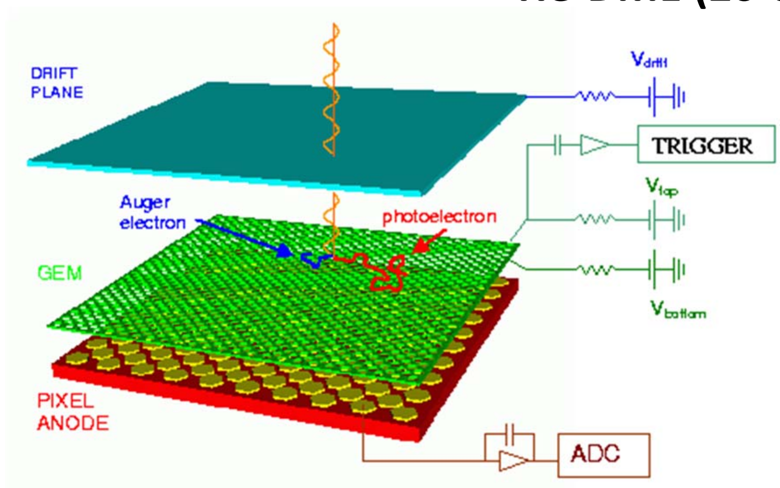

Costa et al., 2001, Bellazzini et al.2006, 2007

GEM electric field

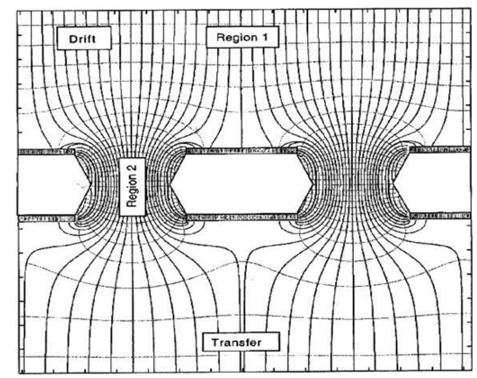

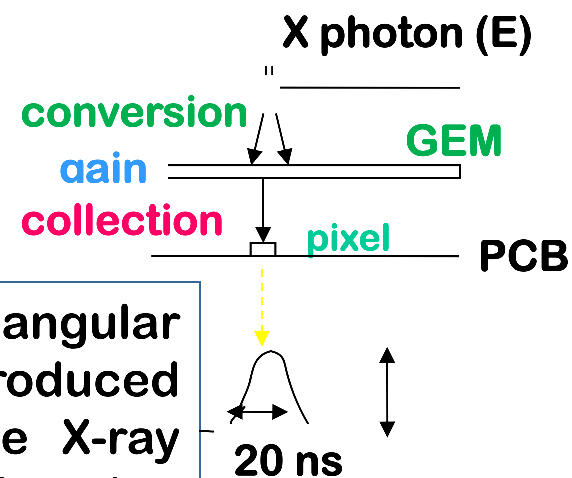

Polarization information is derived from the angular distribution of the emission direction of the tracks produced by the photoelectrons that brings memory of the X-ray polarization. The detector has a very good imaging capability.

ASIC features 105600 pixels 50 μm pitch

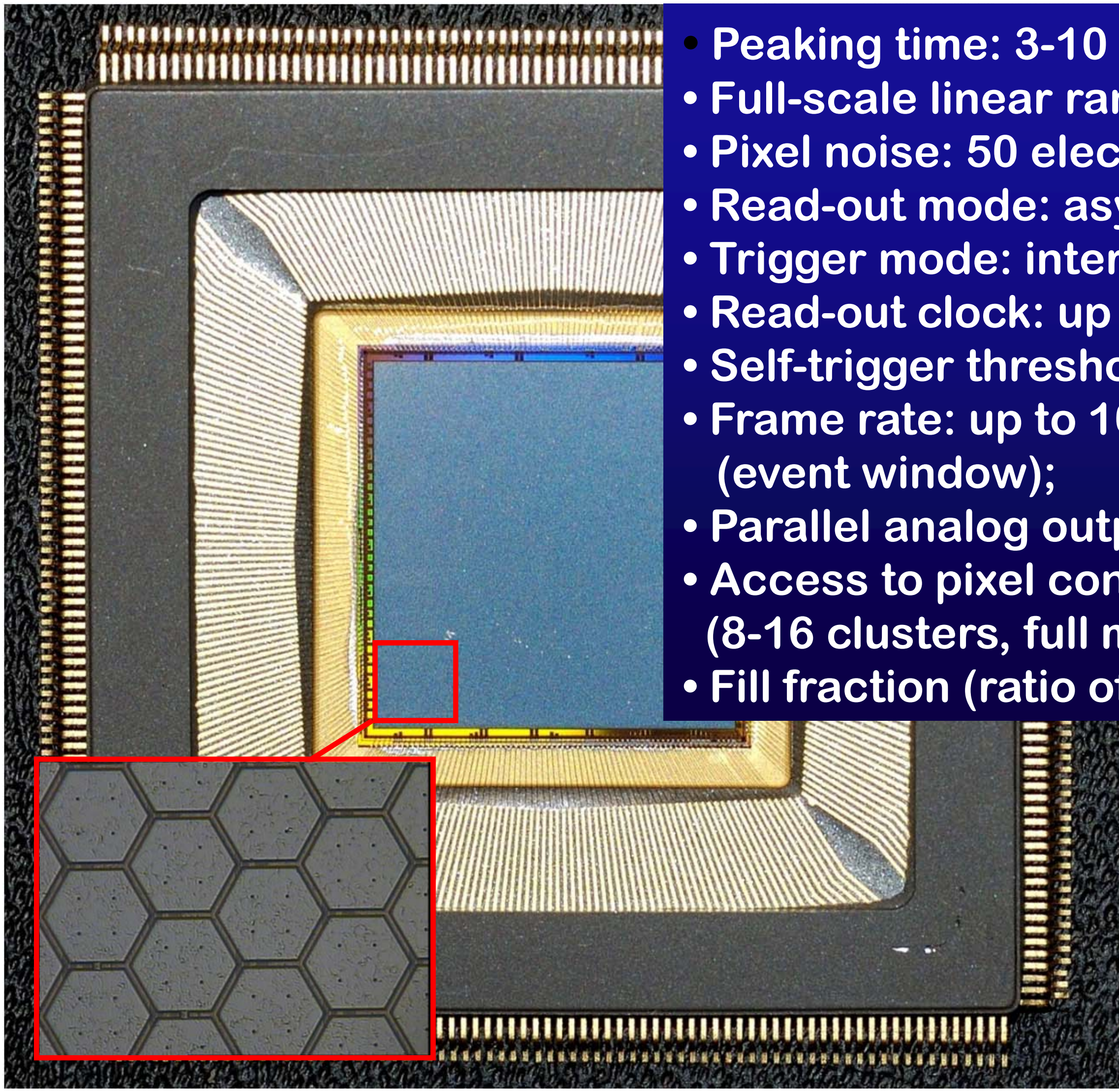

- Peaking time: 3-10 μs, externally adjustable;
- Full-scale linear range: 30000 electrons;
- Pixel noise: 50 electrons ENC;
- Read-out mode: asynchronous or synchronous;
- Trigger mode: internal, external or self-trigger;
- Read-out clock: up to 10MHz;
- Self-trigger threshold: 2200 electrons (10% FS);
- Frame rate: up to 10 kHz in self-trigger mode (event window);
- Parallel analog output buffers: 1, 8 or 16;
- Access to pixel content: direct (single pixel) or serial (8-16 clusters, full matrix, region of interest);
- Fill fraction (ratio of metal area to active area): 92%)

The chip is self-triggered and low noise. The top layer is the collection plane. The bottom 4 layers are a complete analogue chain for each pixel with preamplifier/shaper/sample and hold and serial readout.

It defines the sub-frame that surrounds the track. The dead time downloading an average of 1000 pixels is 100 time lower than for 1E5 pixels.

Tracks analysis

$$\frac{\partial\sigma}{\partial\Omega} = r_o^2 \frac{Z^5}{137^4}\left(\frac{mc^2}{h\nu}\right)^{7/2} \frac{4\sqrt{2}\sin^2(\theta)\cos^2(\varphi)}{(1-\beta\cos(\theta))^4}$$

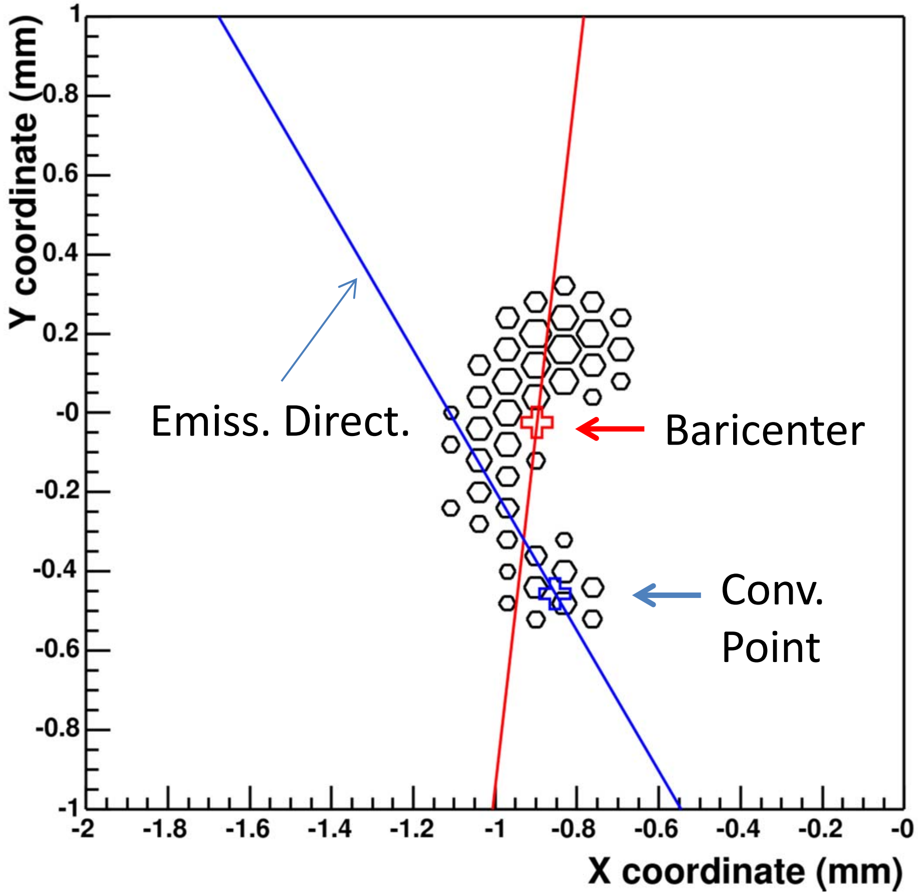

1) **The track is collected by the ASIC.**

2) **Baricenter evaluation (using all the triggered pixels).**

3) Reconstruction of the principal axis of the track: minimization of the second moment of charge distribution.

4) Reconstruction of the conversion point: third moment along the principal axis (asymmetry of charge distribution to select the lower density end) + second moment (length) to select the region for conversion point determination).

5) Reconstruction of emission direction: (minimization of the second moment with respect to the conversion point) but with pixels weighted according to the distance from it.

From the analysis of the track we reconstruct the original direction of the photoelectron (blue line) and the impact point (blue cross).

IAPS-Rome facility for the production of polarized X-rays.

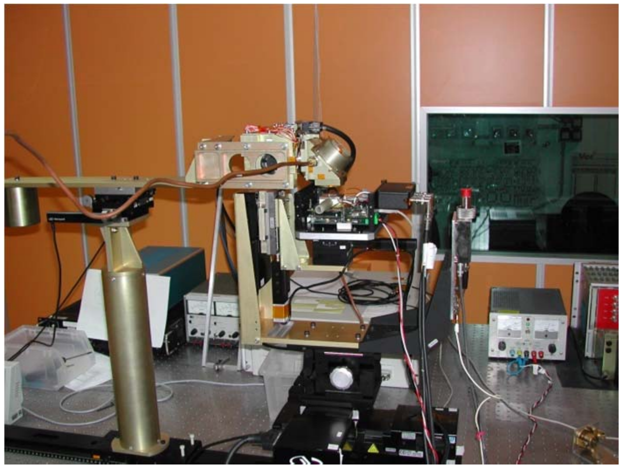

Facility at IASF-Rome/INAF

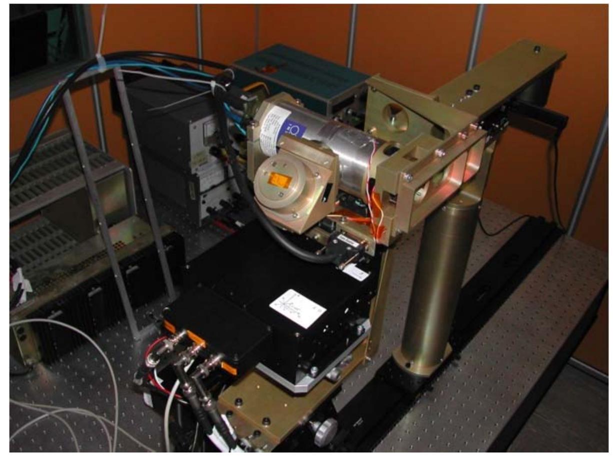

Close-up view of the polarizer and the Gas Pixel Detector

keV	Crystal	Line	Bragg angle
1.65	ADP(101)	CONT	45.0
2.01	PET(002)	CONT	45.0
2.29	Rh(001)	Mo L_α	45.3
2.61	Graphite	CONT	45.0
3.7	Al(111)	Ca K_α	45.9
4.5	CaF_2(220)	Ti K_α	45.4
5.9	LiF(002)	^{55}Fe	47.6
8.05	Ge(333)	Cu K_α	45.0
9.7	FLi(420)	Au L_α	45.1
17.4	Fli(800)	Mo K_α	44.8

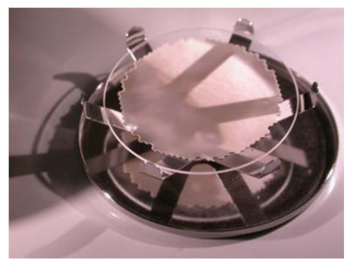

Capillary plate (3 cm diameter)

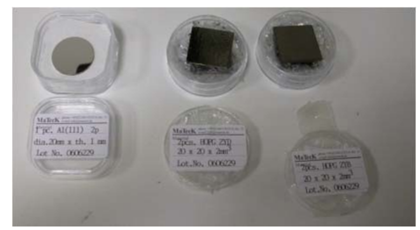

Aluminum and Graphite crystals.

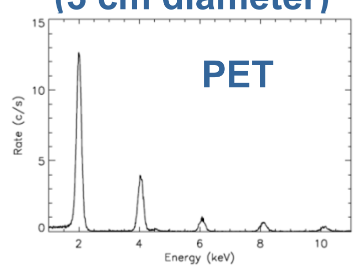

Spectrum of the orders of diffraction from the Ti X-ray tube and a PET crystal acquired with a Si-PiN detector by Amptek

(Muleri et al., SPIE, 2008)

Modulation factor measurements and simulations

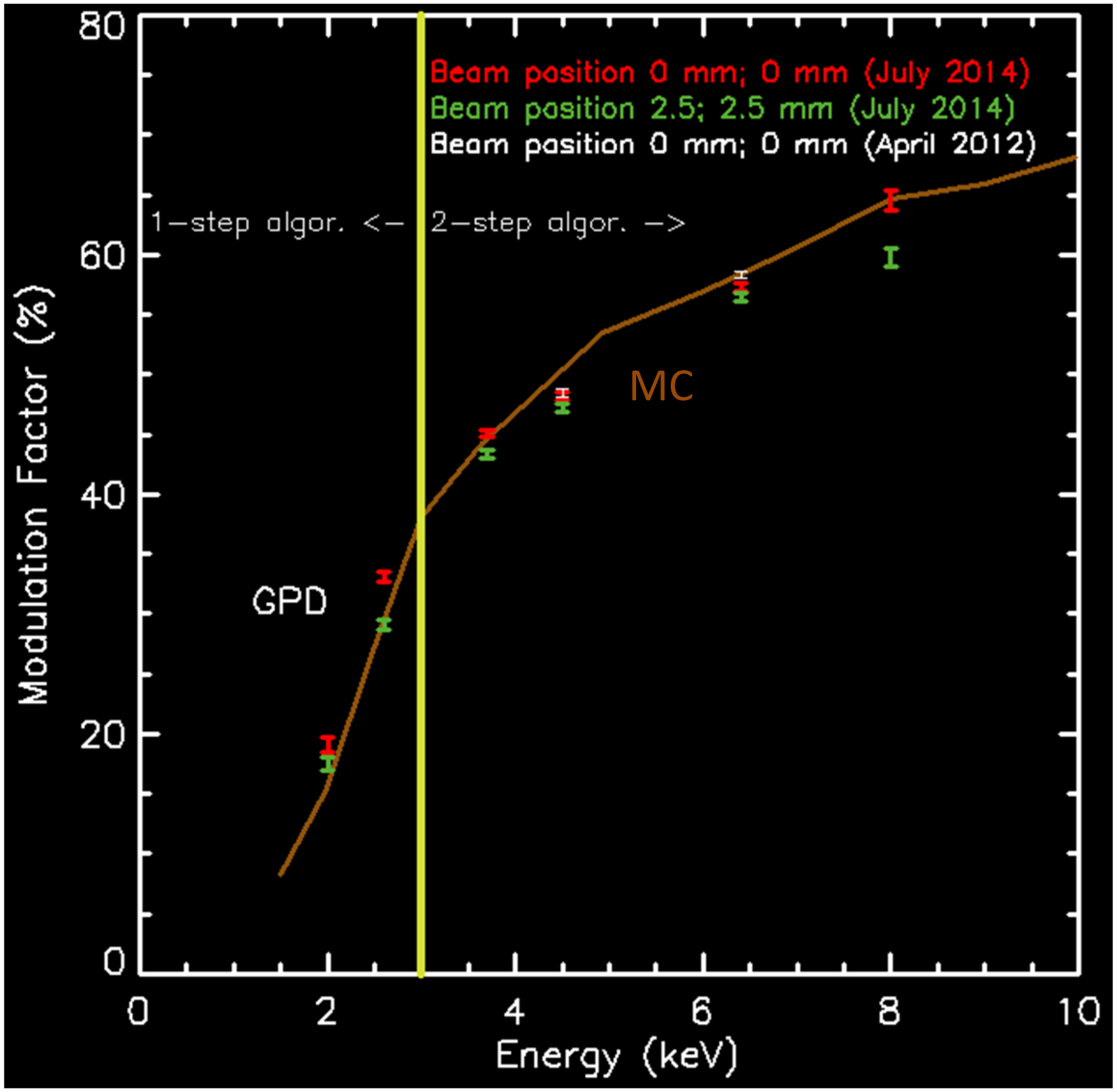

Energy resolution stability of the Low Energy GPD

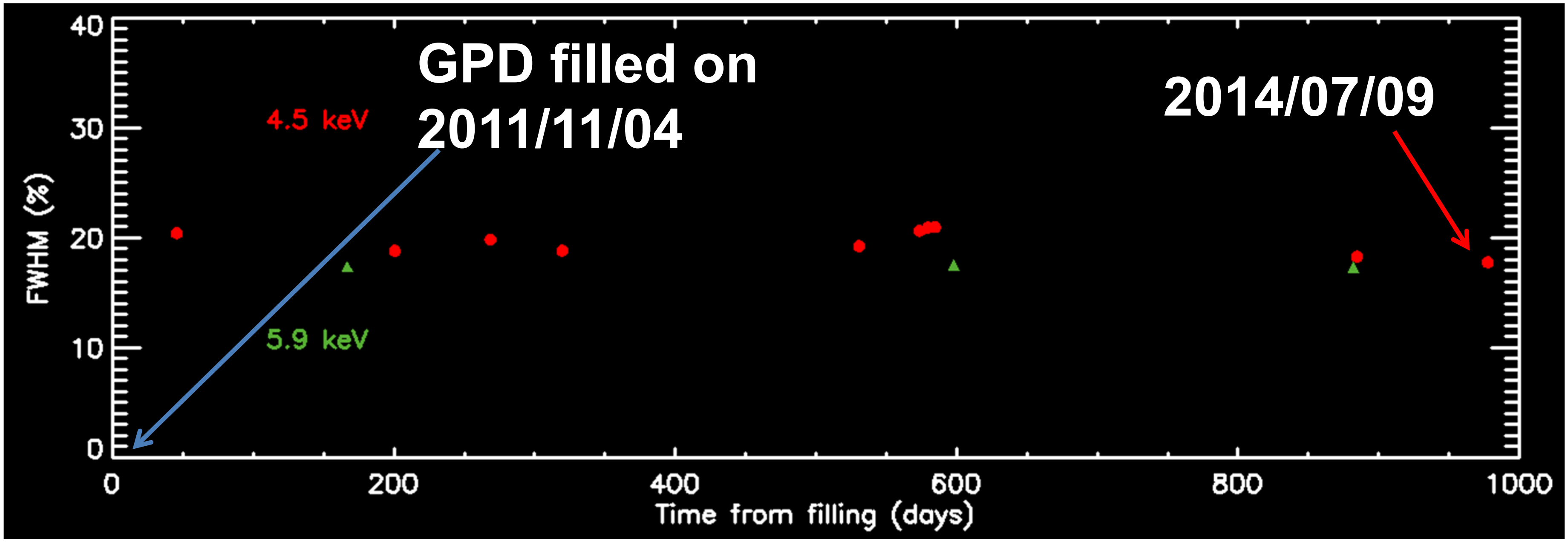

A Gas Pixel Detector for higher energies (6-35 keV)

Current prototype
Argon 70% DME 30% 2 cm, 2 bar

Goal

- Argon mixture @ 3 bar
- Gas cell thickness 3cm
- new ASIC (already being manufactured)
    - Reduce the ROI
    - Increase the clock

Spectroscopy : <20% @ 6 keV
Timing : 8 μs
Dead-Time : 50 μs

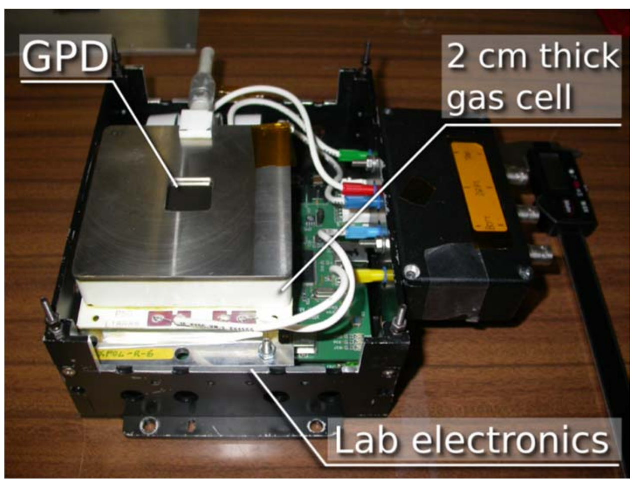

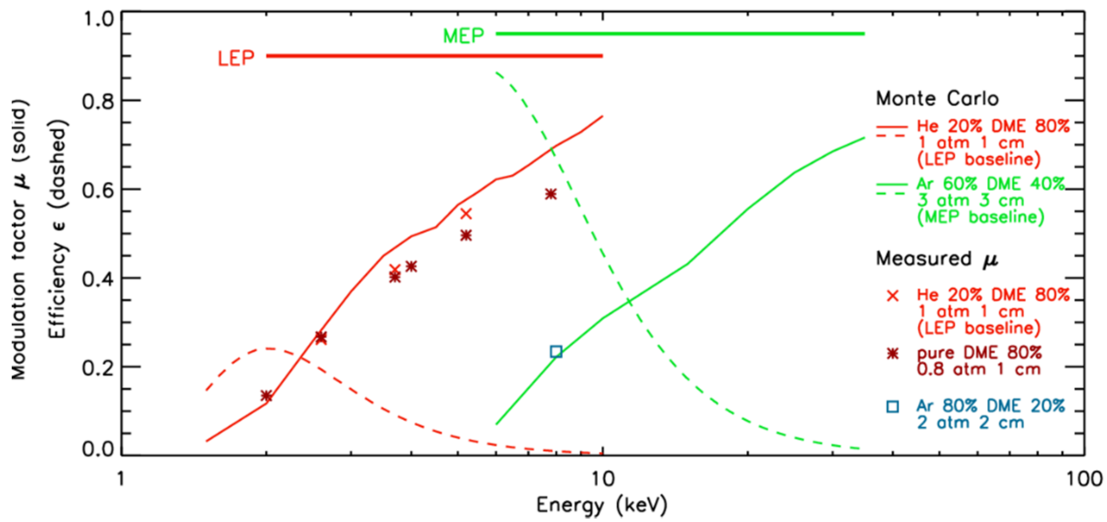

Efficiency (dashed) and modulation Factor (solid) with Monte Carlo and measurement for the **low energy (2-10 keV)** polarimeter and **medium energy (6-35 keV) polarimeter.**

MEP

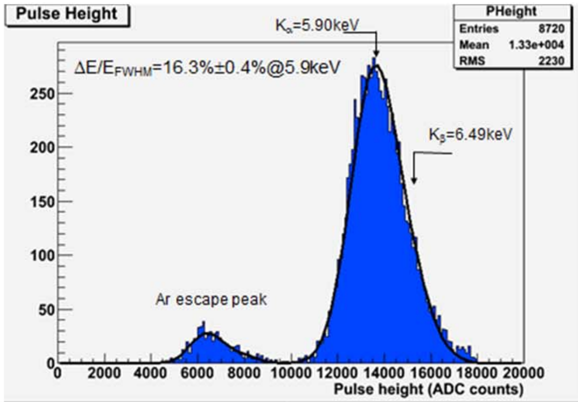

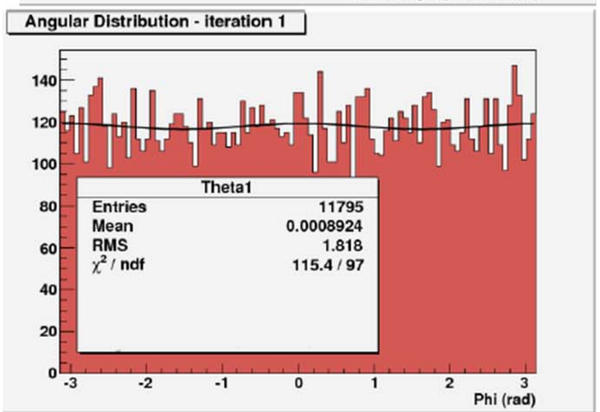

^{55}Fe
Unpol.

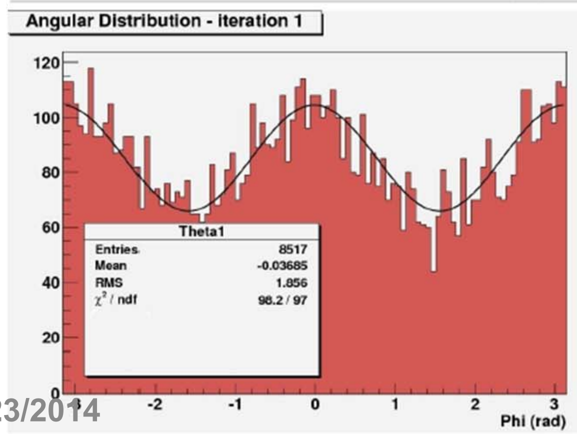

Polarized
9.7 keV

Real tracks @ 22 keV

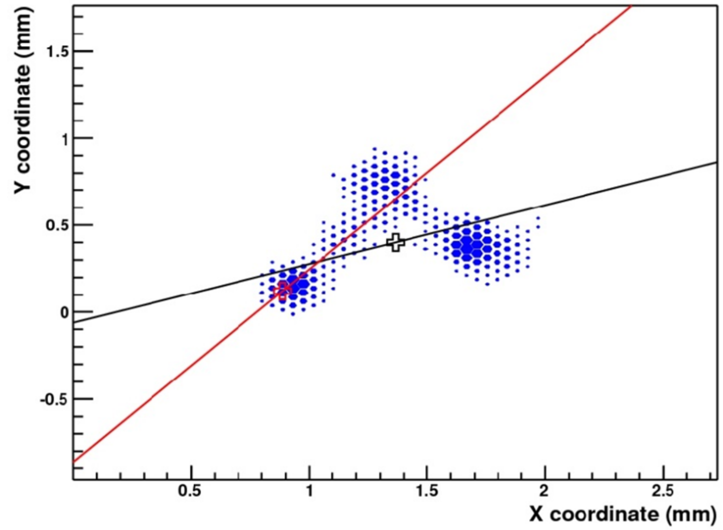

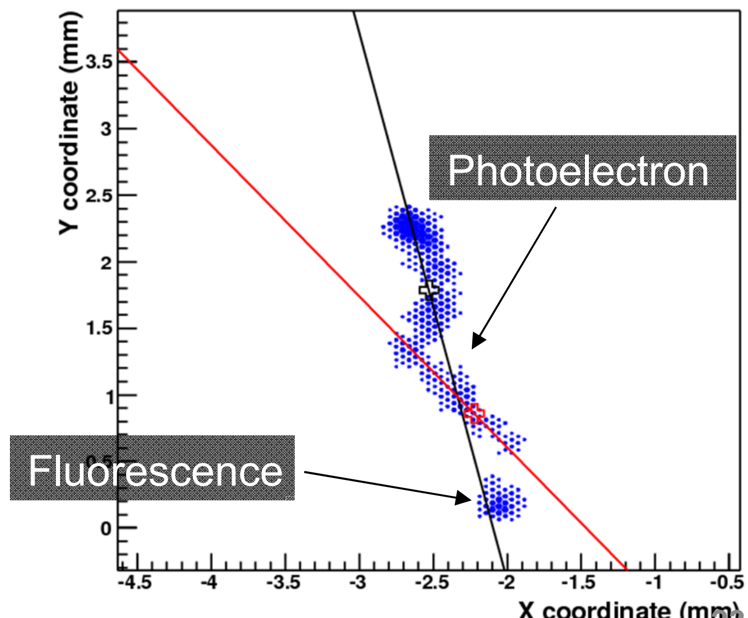

We propose to make a measurement in an energy range starting where the non thermal emission starts to dominate the flare spectrum.

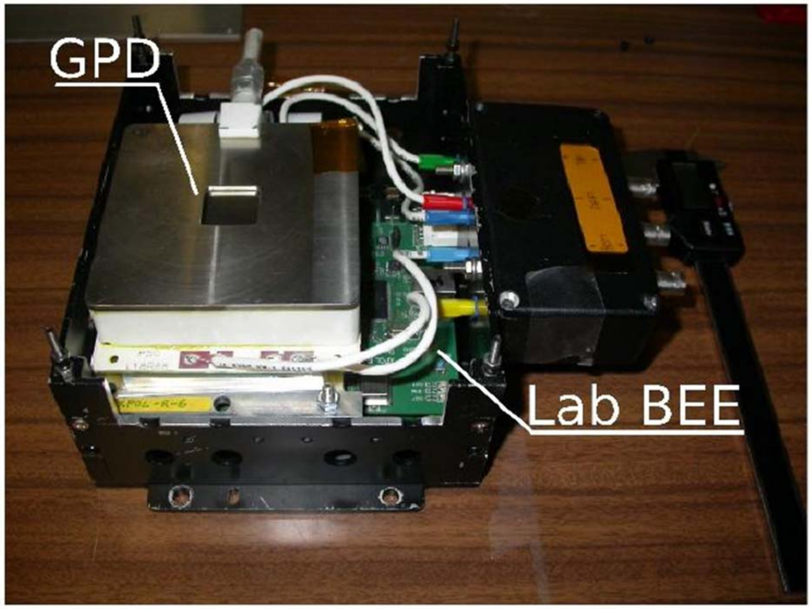

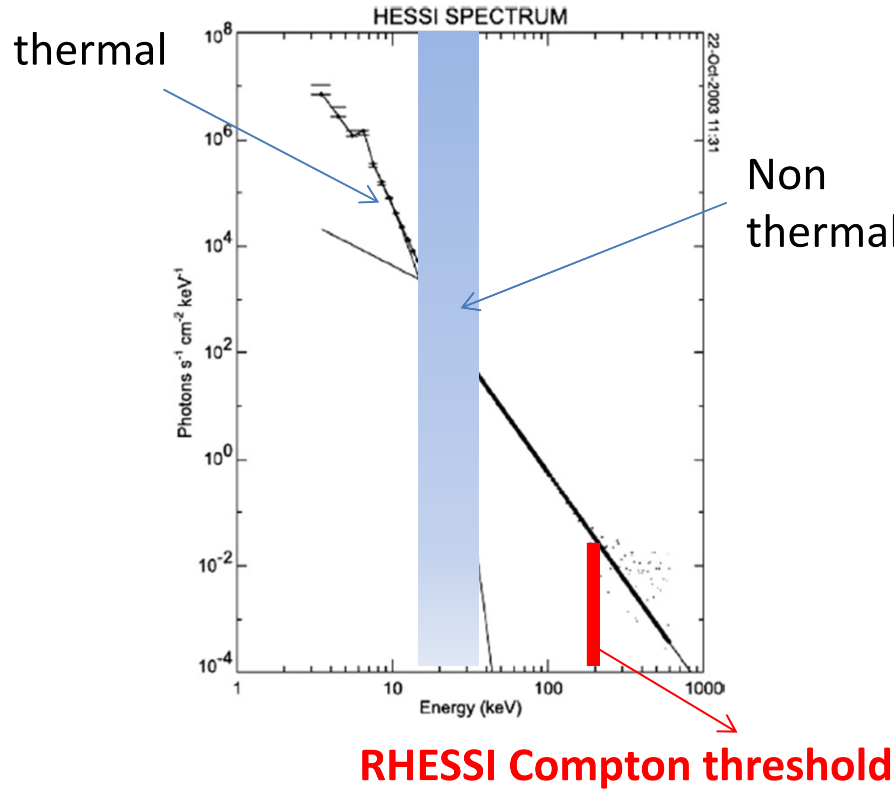

Medium Energy Polarimeter (MEP)
Ar-DME gas mixture
Pressure 3 bar (prototype 2 bar)
Absorption gap thickness 3 cm (prototype 2 cm).

Flare Class	Maximum X-Ray Flux watts per square meter (W/m^2)	Maximum X-Ray Flux ergs per square centimeter per second (erg/cm^2·s)
A*n*	$n \times 10^{-8}$	$n \times 10^{-5}$
B*n*	$n \times 10^{-7}$	$n \times 10^{-4}$
C*n*	$n \times 10^{-6}$	$n \times 10^{-3}$
M*n*	$n \times 10^{-5}$	$n \times 10^{-2}$
X*n*	$n \times 10^{-4}$	$n \times 10^{-1}$

2 MEPs 15-35 keV

Flare class	MDP (%)	Integration time (s)
X10	0.6	748.8
X5.1	1.3	989.4
X1.2	4.8	239.8
M5.2	6.6	489.1
M1	46.4	128.0

Energy Dependent Sensitivity of the SEEPE X-ray polarimeter

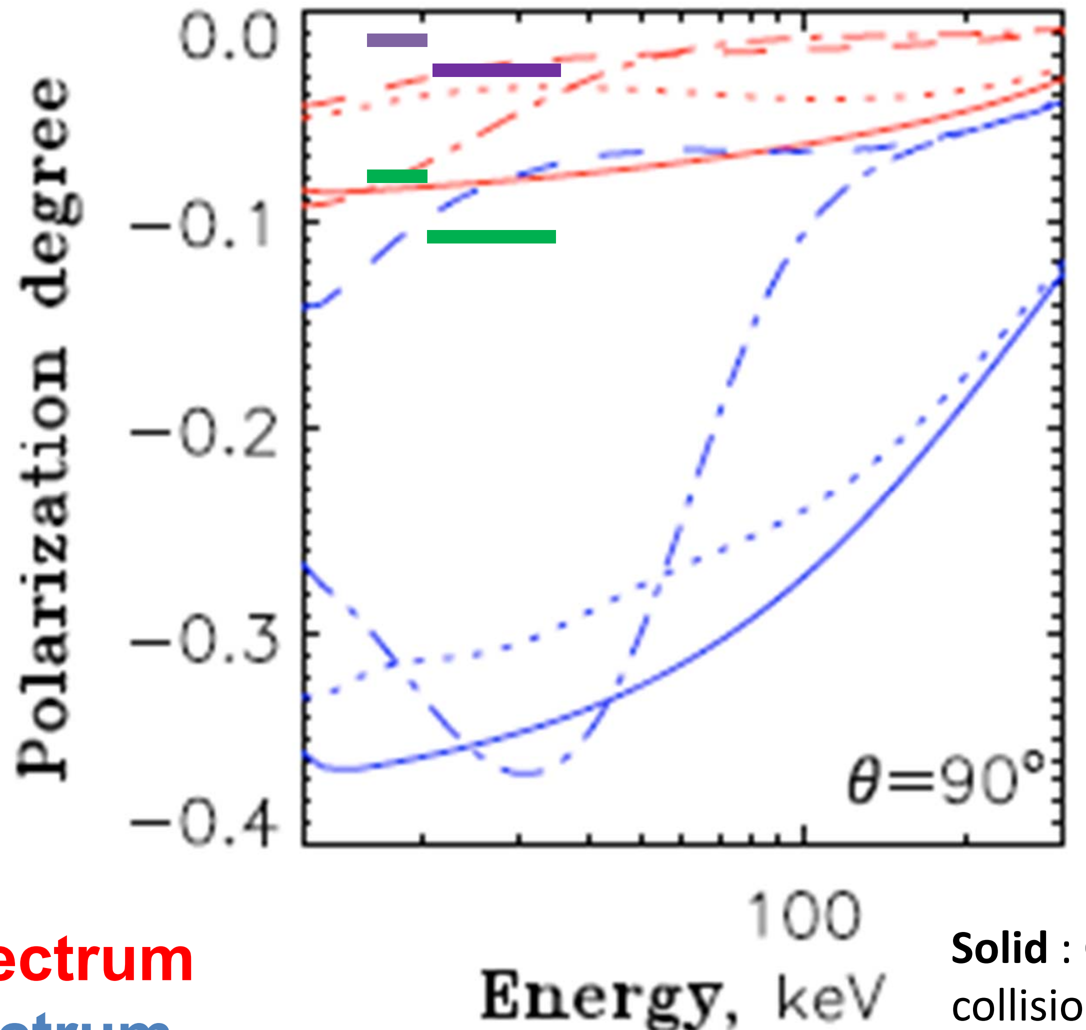

MDP X5.1 Flare

MDP M5.2 Flare

Hard spectrum
Soft spectrum

Model from Zharkova et al., 2010

Solid : Collision; **dotted** collision and return current; **Dashed** : Collision and converging magnetic beam **Dash-dotted** : all

X5.1 Flare

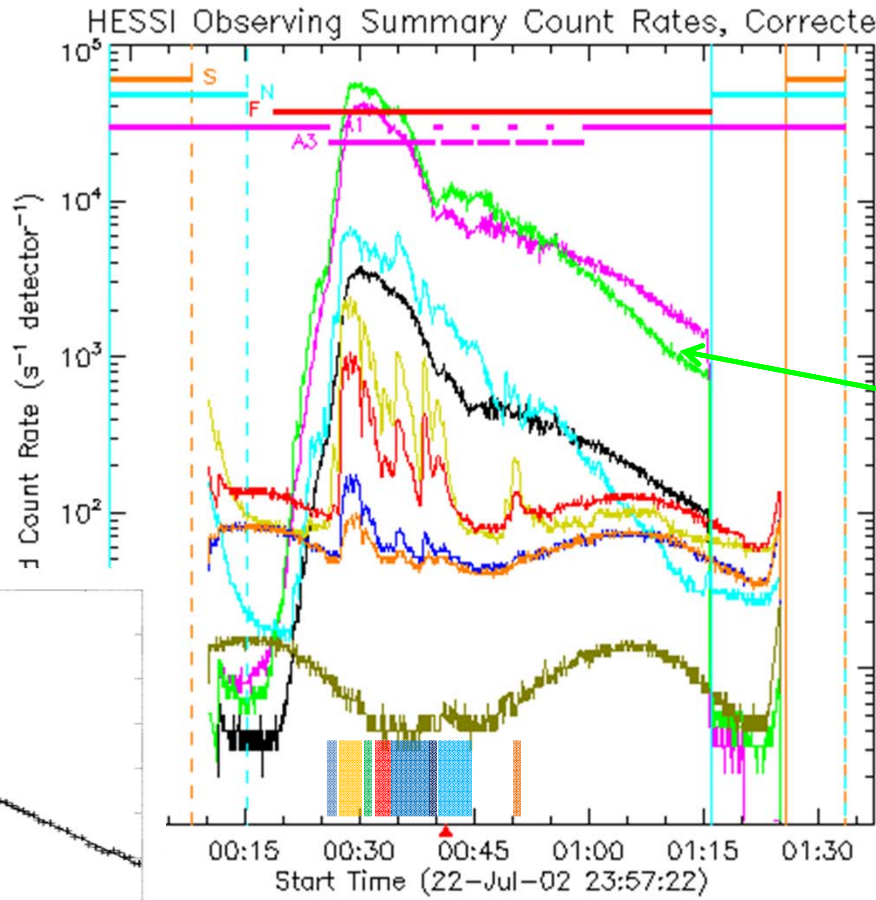

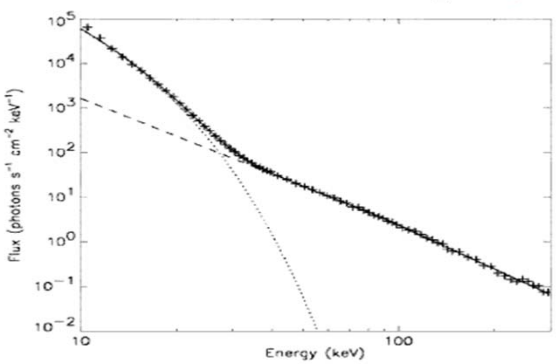

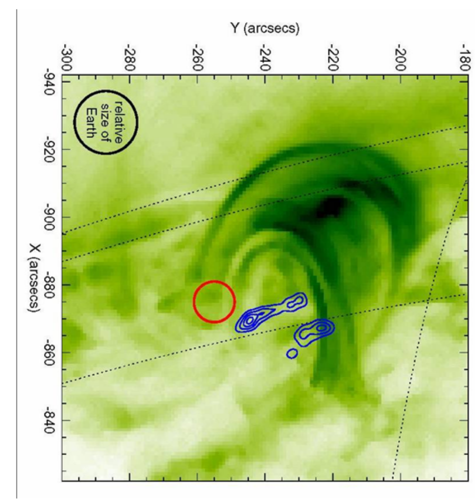

MDP (%) = 4.2 ; 2.4 ; 4.2; 4.6; 3.3; 7.1; 17.9; 25.4

15-35 keV

Scientific Payload

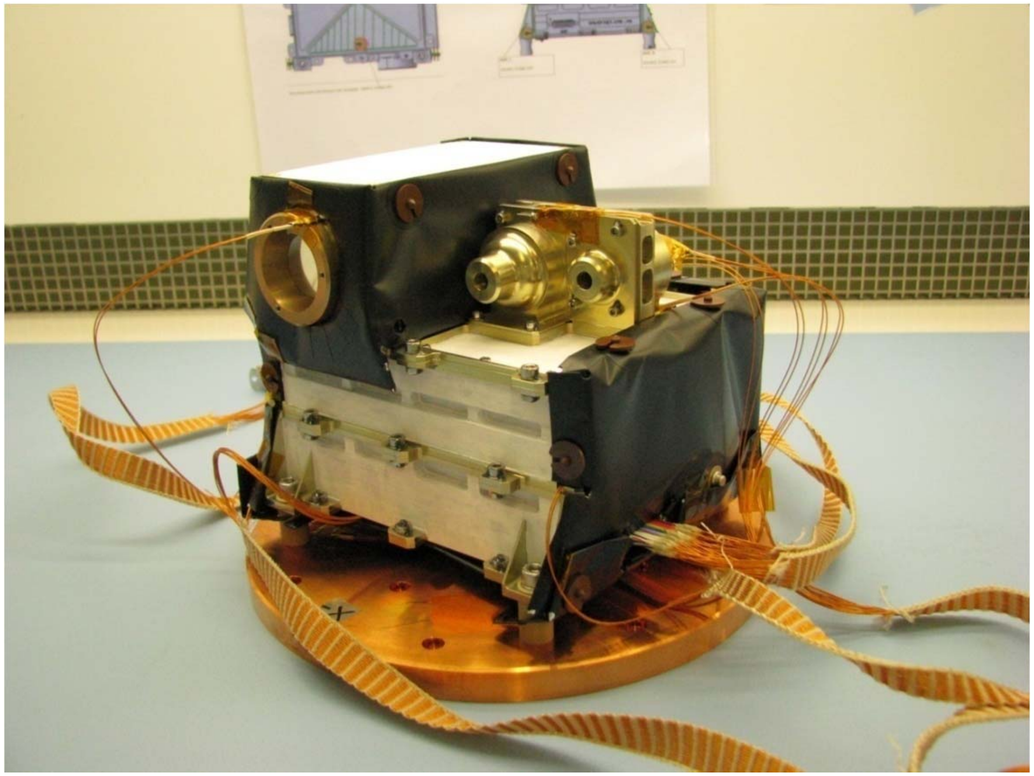

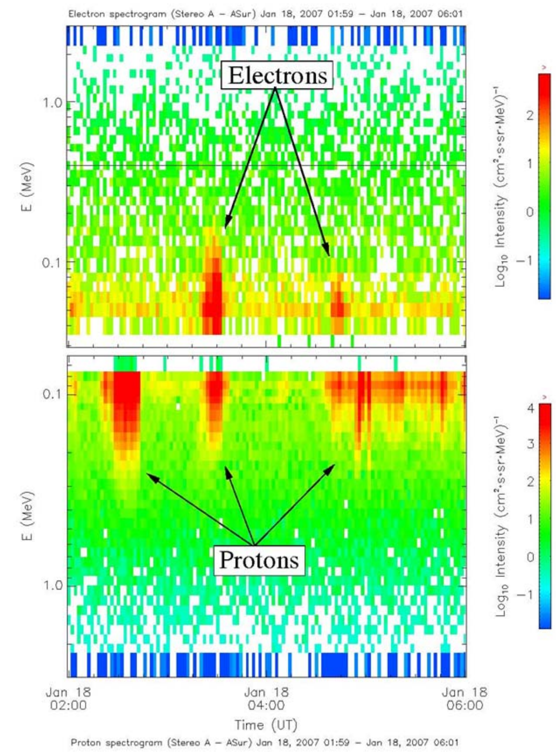

Electron-Proton and High-Energy Telescopes (Transport) (EPT-HET)

Mass	**2.5 kg**
Power	**5 W**
Energy Range	**Electrons: 20 keV – 30 MeV** **Protons: 20 keV – 100 MeV** **Heavy ions: ~10 MeV/nuc – ~200 MeV/nuc (species dependent)**
Time Resolution	**10s (species dependent)**

Scientific Payload

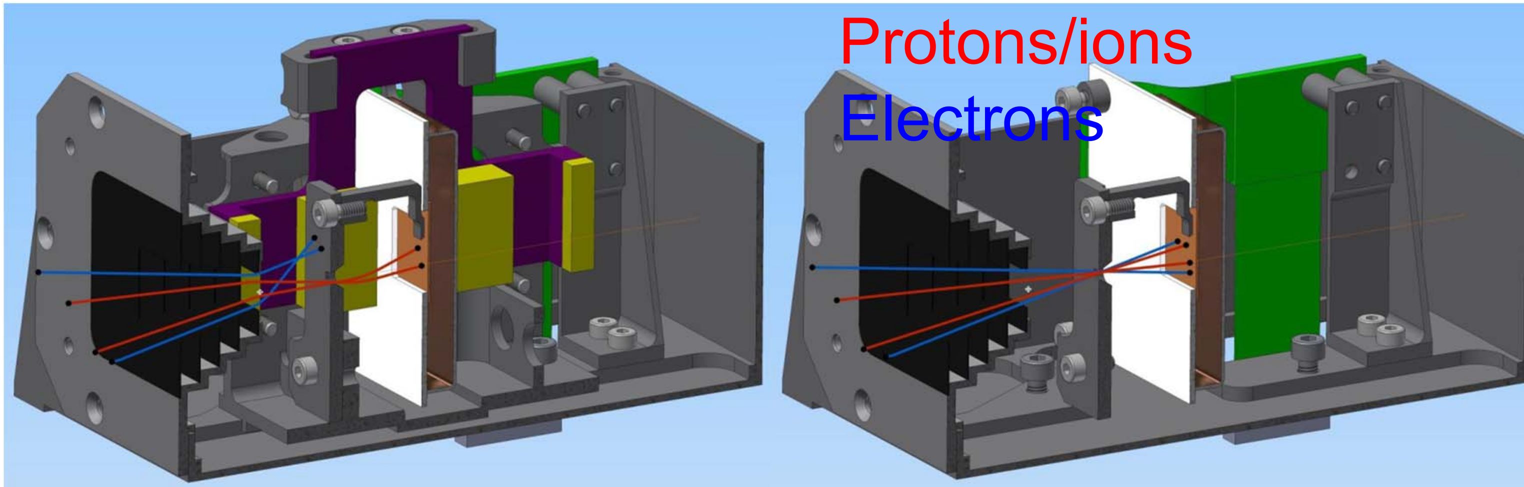

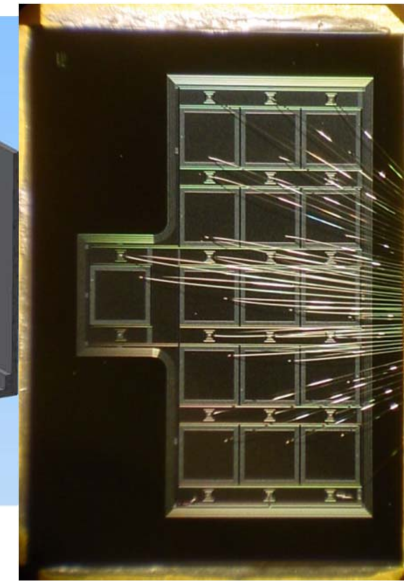

Supra-Thermal Electrons & Protons (STEP)
(Transport, Local Acceleration)

Mass	2.5 kg
Power	5 W
Energy Range	Electrons: 2 keV – 100 keV Protons: 3 keV – 100 keV
Time Resolution	10s (species dependent)

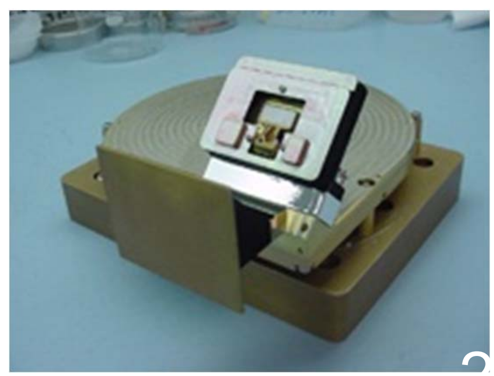

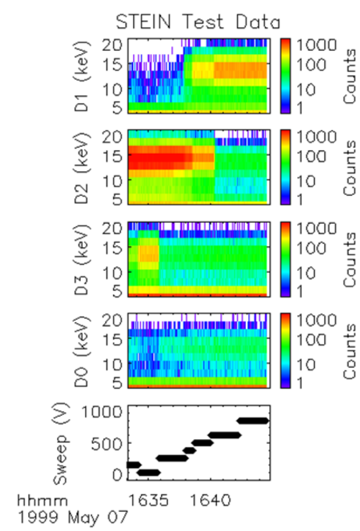

Magnetometer

Linearity Test

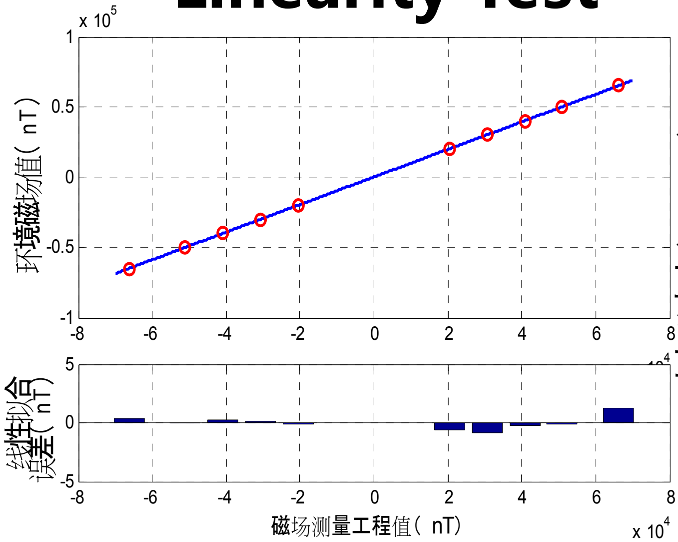

Power Spectrum of Noise

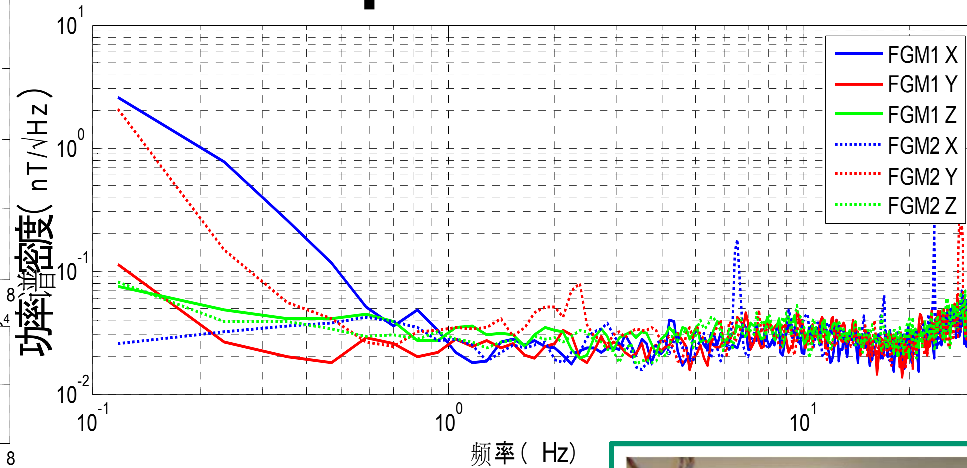

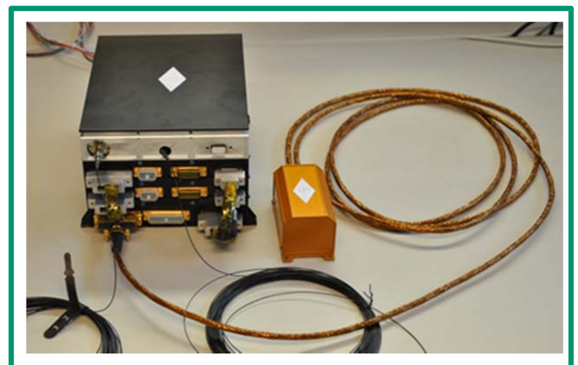

Magnetic Field Range	Better than ±65000nT
noise	<30pT/√Hz @1Hz
mass	1kg
power	<1.5W/detector

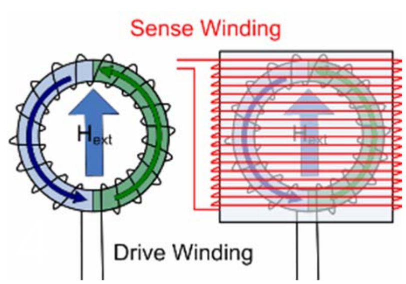

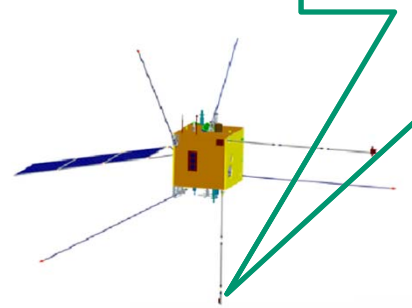

SEEPE

High Energy Band Spectrometer(HEBS)		
Size	362×349×172.5mm	
Weight	20.5 kg	
Power	20 W	
Telemetry	2 GB/day	
Energy Range	10keV - 600MeV	
Energy Resolution	3%@662keV	
Temporal Resolution	1s(quiescent),32ms (flare-mode)	
Effective Area	>60cm^2@1MeV	
Sensitivity (300keV-10MeV)	Better than 3X10^{-3}photos/cm^2/s	
X-ray Polarimeter (Gas Pixel Detectors)		
Weight	16 kg	
Power	25 W	
Energy Range	10-35keV(for non-thermal bremsstrahlung)	
Mass Memory	2.5 GB to be downloaded sporadically (1-2 /month)	
Electron and Ion Detectors		
	EPT-HET	STEP
Mass	2.5 kg	2.5 kg
Power	5 W	5 W
Telemetry	1.5 kbps	1 kbps
Energy Range	Electrons: 20 keV – 30 MeV Protons: 20 keV – 100 MeV Heavy ions: ~10 MeV/nuc – ~200 MeV/nuc (species dependent)	Electrons: 2 keV – 100 keV Ions: 3 keV – 100 keV
Time Resolution	10s (species dependent)	10s
Geometry Factor [cm^2 sr]	EPT: 2 x 0.01 HET: 3 x 0.21 (protons) HET: 2 x 0.26 (heavy ions)	2 x 1.7 10^{-4} or 2 x 7.5 10^{-3}
Magnetometer		
1kg	1.5W/detector	±65000nT

Total:
43.5 kg
56.5 W

Launcher and Orbit

Plan	One	Two
Orbit	~700km	Lunar Resonance
Launcher	Long March 2	Vega or equivalent with propulsion module.
Cost	~10M Euro (1st institute)	Under study
Bus	~10M Euro (DongFangHong or Shanghai Mini-satellite institute)	CGS/OHB/under study.
Issues	Without Particle Detectors and Magnetometer	more complicated mission profile, more resources needed for the spacecraft, included satellite transmission.

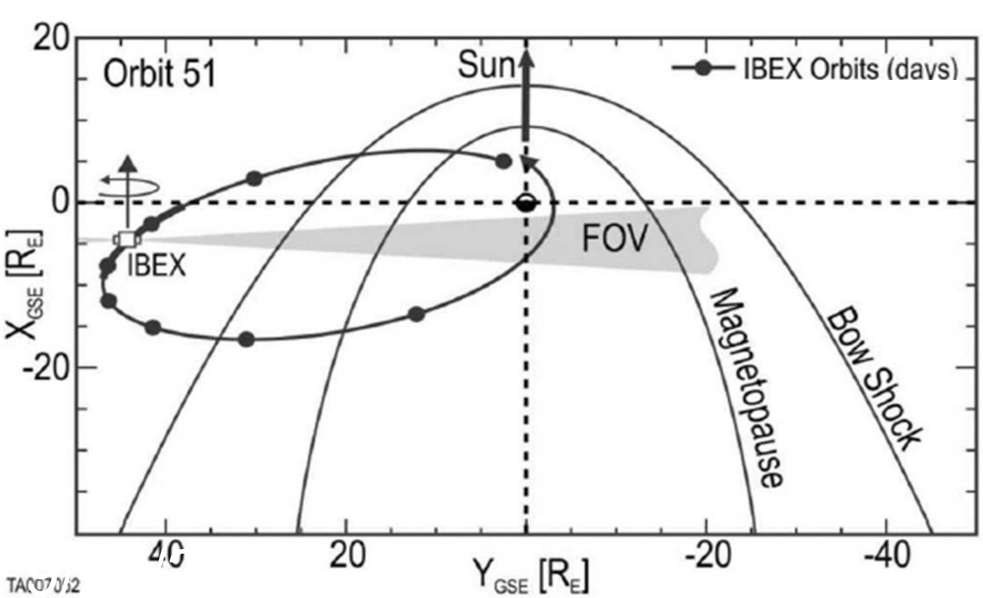

An example of platform that among others is compliant with the mission requirements.

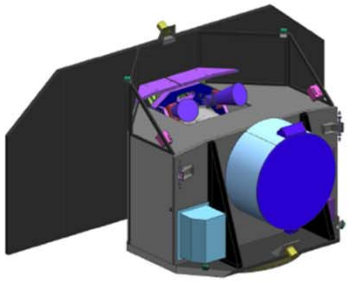

OHB CGS

SB 200 SATELLITE PLATFORM

Parameter	Value
Orbit	from 600 to 1050 km for SSO
Max payload mass	up to 70 kg
Payload envelope (h; w;l)	Cylindrical shape with an envelope of Ø 0.64 m x L 1.3 m
Average payload power	60 W
Max Bus dry mass (Hydrazine)	159 kg; (13 kg)
Pointing accuracy (control)	2.2 arcmin
Attitude determination (knowledge)	50 arcsec
Pointing stability (drift)	1 arcsec/s
Maximum Radiation total dose	10 krad
TC&R desciption, frequency band and rates	S band DWLK: 2,29 GHz for 570 Kbps; Sband UPL:2,1 4 kbps X band transmisison could be implemented

SEEPE

Schedule

- Mission selection: 2014-2015
- Study phase: 2016-2017
- Implementation phase: 2018-2021
- Launch: 2021

The next solar cycle starts near 2021!

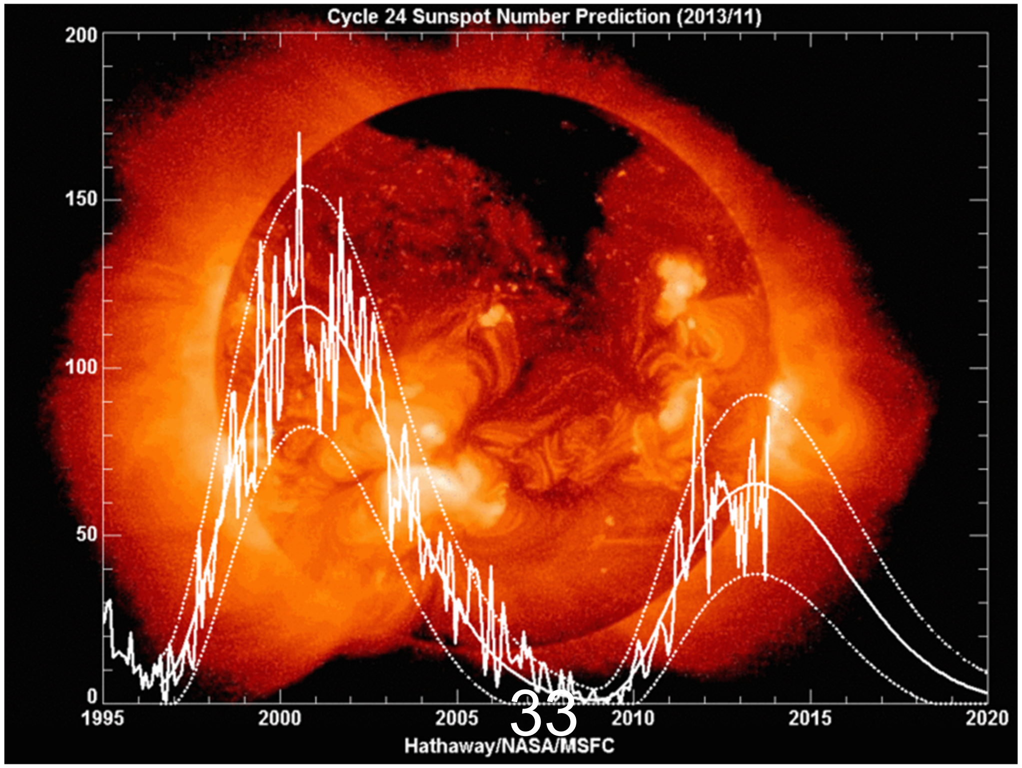

Complementary Missions

- SDO (2010-)
- IRIS (2013-)

Magnetic Fields.

Thermal Emission.

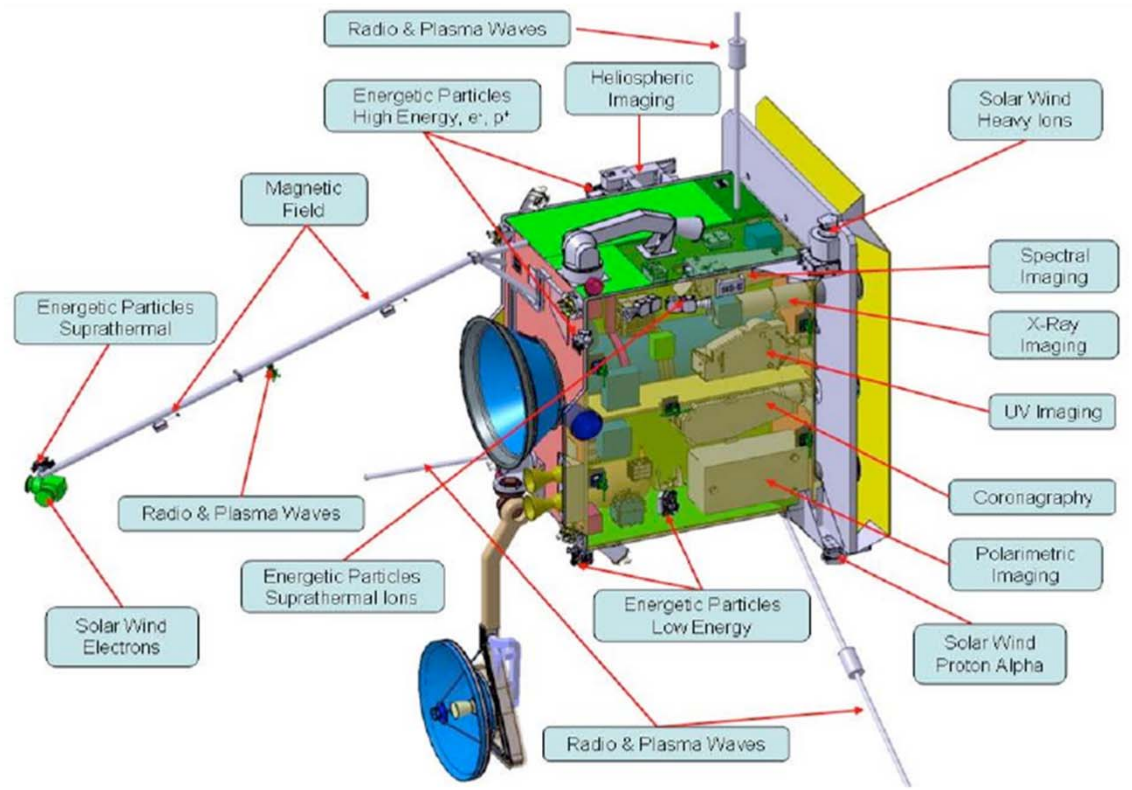

- Solar Orbiter
- Solar Probe +

(~2018-)

<0.3 AU.

STIX: X-ray Images; EPD: electrons, protons, ions.

Solar Wind Electrons Alphas and Protons Investigation.

- Advanced Solar Obs. (2020-) 1.0AU, X-ray Imager.

Complementary Observations

- Radio

  Gyro-synchrotron and Bremsstrahlung

  Magnetic Fields, Energetic Electron Beams

- Hα

  Irradiation by X-ray and Heating by energetic particles

- Optical (ATST)

  Energetics of thermal and non-thermal particles

Team

Science and Data Analysis:

Siming Liu, Youping Li, Weiqun Gan (PMO, CAS), Linghua Wang (PKU), Gang Qin (NSSC), Chuan Li (NJU), China, Valentina Zharkova Northumbria University, Newcastle, UK, Giovanni Peres, Fabio Reale (Universita' di Palermo), IT

High Energy Band Spectrometer:

Jian Wu, Jin Chang Purple Mountain Observatory, China

X-ray Polarimeter:

Paolo Soffitta, Enrico Costa, Sergio Fabiani, Fabio Muleri Istituto Di Astrofisica e Planetologia Spaziali (IAPS)
Ronaldo Bellazzini, Alessandro Brez, Massimo Minuti, Michele Pinchera, Gloria Spandre (INFN-Pisa)

Electron-Proton and High Energy Telescopes and STEP:

Robert F. Wimmer-Schweingruber Institut fuer Experimentelle und Angewandte Physik, University of Kiel, Germany

Magnetometer:

Yong Liu National Space Science Center, CAS, China

Summary

Solar Energetic Emission and Particles Explorer (SEEPE) is a timely mission suitable for the ESA and CAS joint scientific space mission:

1) The proposed mission meets the boundary conditions and draws on expertise in both China and Europe;

2) The scheduled launch time matches the onset of the next (25^{th}) solar cycle;

3) It is highly complementary to the ESA's Solar Orbiter, NASA's Solar Probe Plus, CAS's ASO missions for the 25^{th} solar cycle;

4) The timing, spectral, polarization, and energetic particles observations of the solar activity, in coordination with other ground and space based observations, will help to reveal how the space weather is driven by the Sun.

Solar flare mechanisms

only reconnection can account for directivity of accelerated particles

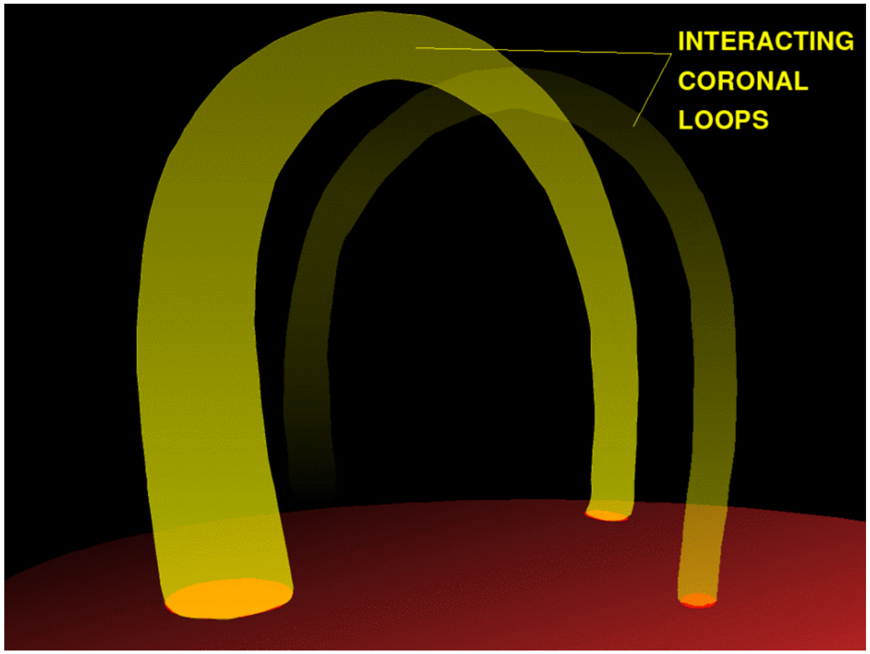

Cartoon of coronal loops

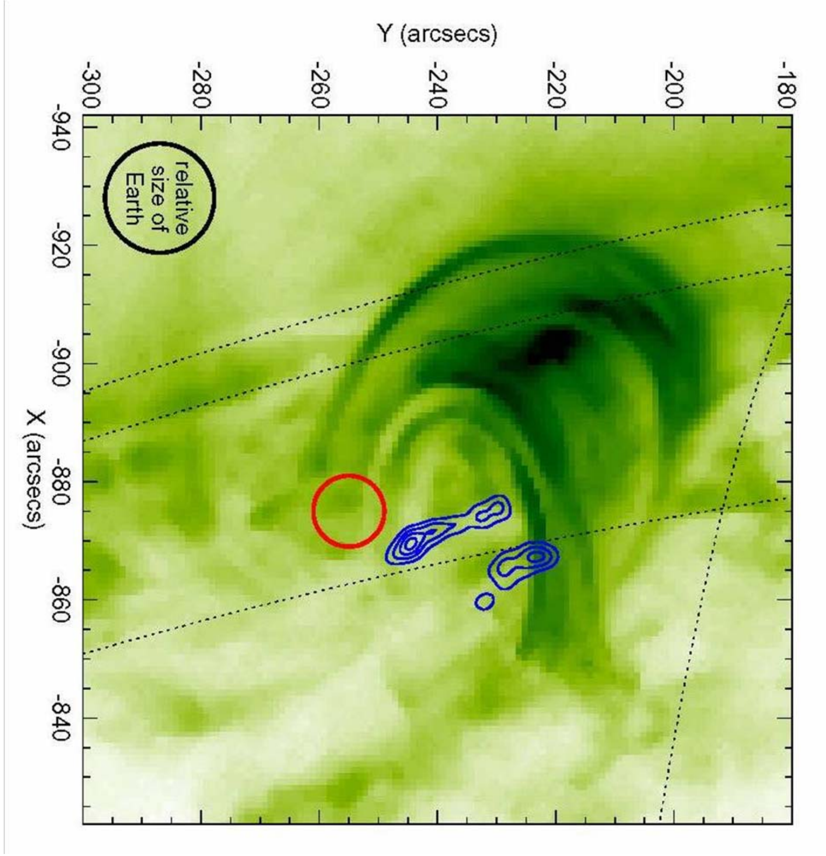

Real image of coronal loops

The presence of hard X-ray emission and gamma emission at the bottom of coronal loops indicates the presence of highly directed electrons and protons in solar flares.

Evolution of photon spectrum and polarization degree spectrum for photons at $\vartheta = 90^o$ with respect to B for soft and hard electron beam

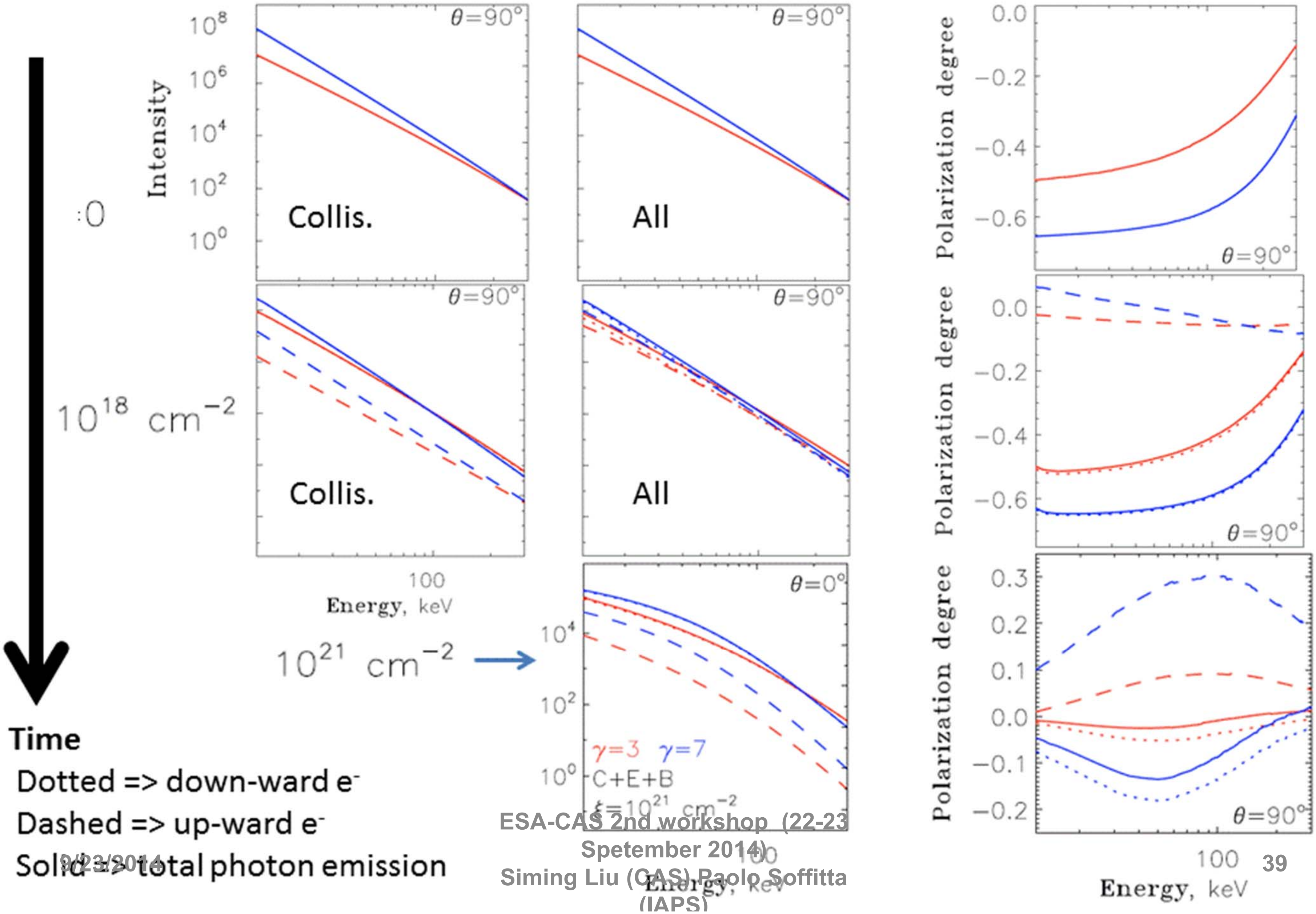

Particle in cell simulation
(PIC, Siverski and Zharkova 2009)

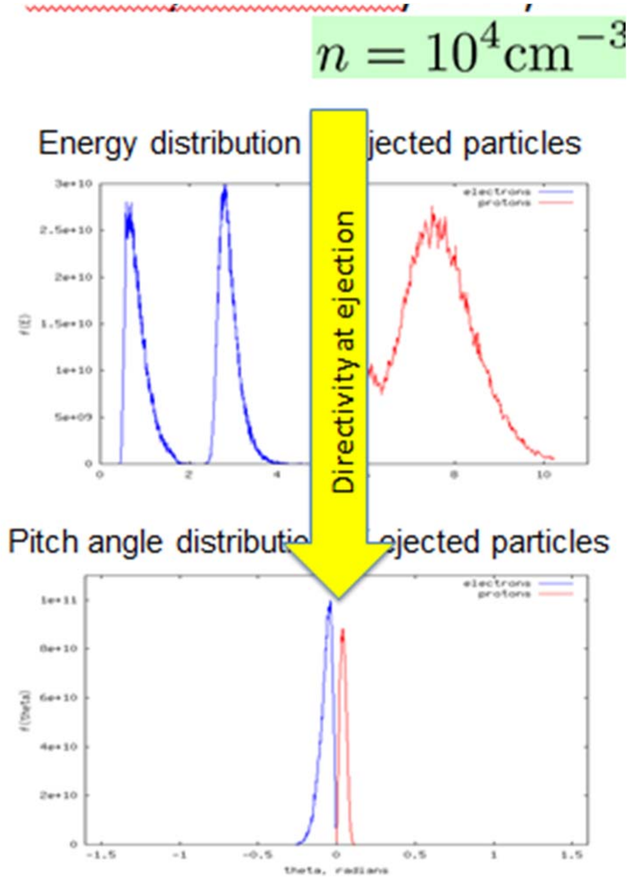

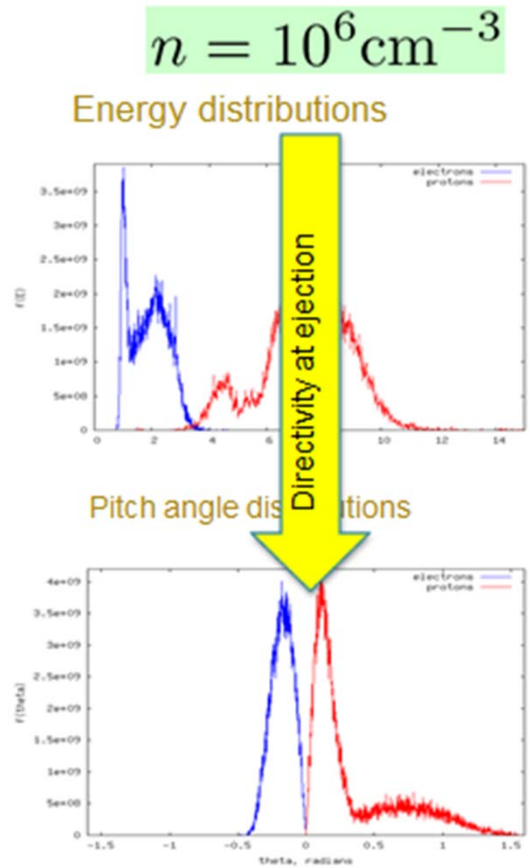

Simulations reveal that, during acceleration appears a polarisation electric field which is responsible for separating electron from proton with narrow pitch angle (p.a, angle between the B and v of particles, positive cosine downward) distribution.

Photoelectric effect

Polarimetry based on photoelectric effect was tempted very long ago but it is now a mature technology.

Heitler W.,The Quantum Theory of Radiation

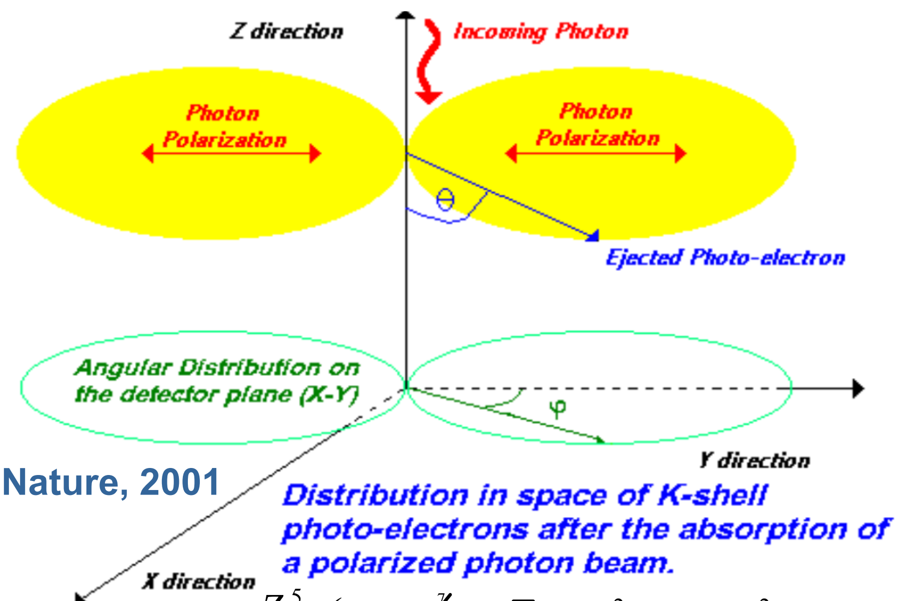

Costa, Nature, 2001

$\beta = v/c$

$$\frac{\partial\sigma}{\partial\Omega} = r_o^2 \frac{Z^5}{137^4}\left(\frac{mc^2}{h\nu}\right)^{7/2} \frac{4\sqrt{2}\sin^2(\theta)\cos^2(\varphi)}{(1-\beta\cos(\theta))^4}$$

By measuring the angular distribution of the ejected photoelectrons (the modulation curve) it is possible to derive the X-ray polarization.

An X-ray photon directed along the Z axis with the electric vector along the Y axis, is absorbed by an atom.

The photoelectron is ejected at an angle θ (the polar angle) with respect the incident photon direction and at an azimuthal angle φ with respect to the electric vector.

If the ejected electron is in 's' state (as for the K–shell) the differential cross section depends on cos² (φ), therefore it is preferentially emitted in the direction of the electric field.

Being the cross section always null for φ = 90º the modulation factor μ equals 1 for any polar angle.

Hard X-ray polarimetry as a diagnostic of electron beams precipitating from the corona down to the solar chromosphere

Slides extracted from and with the help of
Valentina Zharkova.

Material from :

Siversky, T.V. & Zharkova V.V., A&A, 2009

Siversky, T.V. & Zharkova V.V., JPP, 2009

Zharkova V.V., Kuznetsov A.A., & Siversky T.V., A&A, 2010